Top Organomet Chem (2017) 60: 113–152
DOI: 10.1007/3418_2016_11

Published online: 9 February 2017

Synthetic Nitrogen Fixation with Mononuclear Molybdenum(0) Phosphine Complexes: Occupying the *trans*-Position of Coordinated N_2

Nadja Stucke, Thomas Weyrich, Mareike Pfeil, Katharina Grund, Andrei Kindjajev, and Felix Tuczek

Abstract Synthetic nitrogen fixation with molybdenum phosphine complexes has witnessed a renaissance recently due to the discovery that such systems are competent to catalytically convert N_2 to ammonia. In the framework of this research area, we have prepared complexes of the type $[Mo(N_2)(PEP)(P_2)]$ (E = N, P; P_2 = dppm, dmpm) in which the linear PEP ligand coordinates in a facial geometry. Similar complexes have been prepared using mixed carbene–phosphine (PCP) ligands. Furthermore, molybdenum bis(dinitrogen) complexes have been synthesized which are facially coordinated by a tripod ligand and contain the bidentate coligands dppm and dmpm. Recently, both of these approaches have been united in the synthesis of a Mo(0)–N_2 complex supported by a pentadentate tetrapodal (pentaPod) ligand. The structural, electronic, and vibrational properties of all of these dinitrogen complexes have been investigated by NMR, IR, and Raman spectroscopy, and their reactivities in a nitrogen fixing cycle have been evaluated. To this end, protonated derivatives have been investigated as well. On the basis of these results and DFT calculations, these systems are promising candidates for the catalytic conversion of N_2 to ammonia.

Keywords Mixed phosphine/carbene ligands • Molybdenum complexes • Multidentate phosphine ligands • Nitrogen fixation

Contents

1 Introduction 114
2 Mo(0)–Dinitrogen Complexes Supported by Tridentate PEP Ligands (E = P, N) 115

N. Stucke, T. Weyrich, M. Pfeil, K. Grund, A. Kindjajev, and F. Tuczek (✉)
Institute of Inorganic Chemistry, Christian Albrechts University Kiel, Max-Eyth-Str. 2, 24098 Kiel, Germany
e-mail: ftuczek@ac.uni-kiel.de

3 Mo(0)–Dinitrogen Complexes Supported by Mixed Imidazol-Ylidene/Phosphanyl Hybrid Ligands 119
4 Mo(0)–Dinitrogen Complexes Supported by Tripodal Ligands with Aryl Substituents 130
5 Mo(0)–Dinitrogen Complexes Supported by Hybrid Tripodal Ligands with Mixed Dialkylphosphine/Diarylphosphine Donor Groups 135
6 Mo(0)–Dinitrogen Complexes Supported by Tetradentate NP_3 Ligands 139
7 Mo(0)–Dinitrogen Complex Supported by a Pentadentate Tetrapodal Phosphine ($pentaPod^P$) Ligand 144
8 Summary and Conclusion 149
References 150

1 Introduction

One of the grand challenges of biological, inorganic, and organometallic chemistry is the conversion of molecular dinitrogen to ammonia under ambient conditions [1]. In nature, this process is catalyzed by the enzyme nitrogenase according to the equation [2]:

$$N_2 + 8H^+ + 8e^- + 16MgATP \rightarrow 2NH_3 + H_2 + 16MgADP + 16P_i$$

This process is highly energy consuming [3], and during the reduction not only ammonia but also H_2 is developed. Nitrogenase consists of two proteins. The larger one, called molybdenum–iron (MoFe) protein, is an $\alpha_2\beta_2$-tetramer which contains two iron–sulfur clusters, the P-clusters, and two iron–molybdenum cofactors (FeMoco) which are the active site of the enzyme where the reduction of dinitrogen occurs [4–7]. The electrons needed are provided by the iron (Fe) protein by forming a complex with the MoFe protein. One electron is transferred from the Fe protein; then the Fe protein dissociates and is recharged, so it is able to reduce the MoFe protein again. After accomplishing this process eight times, one catalytic cycle is completed [8].

Dinitrogen can also be converted to ammonia under ambient conditions by transition metal complexes [9, 10]. In the last years, synthetic model systems have been established that even allow a catalytic ammonia synthesis in a nitrogenase-like fashion with turnover numbers of up to 60 per mononuclear catalytic metal site [11, 12]. The earliest of these systems was discovered by Schrock and coworkers in 2003 and is based on a molybdenum complex with a sterically shielding $HIPTN_3N$ ligand ($HIPTN_3N = [\{3,5\text{-}(2,4,6\text{-}i\text{Pr}_3C_6H_2)_2C_6H_3NCH_2CH_2\}_3N]^{3-}$) [13, 14]. Using decamethylchromocene as reductant and lutidinium BAr^F (BAr^F = tetrakis[3,5-bis (trifluoromethyl)phenyl]borate) as proton source, ammonia was generated from N_2 with this system in four cycles with an overall yield of 65% [14]. A few years later, Nishibayashi et al. established a dinuclear molybdenum–dinitrogen complex supported by a PNP-pincer ligand [15–17]. With a combination of decamethylcobaltocene and lutidinium triflate, this system generated 12 equiv. NH_3 per molybdenum center. Most recently, the original catalyst was modified by applying tridentate triphosphine ligands instead of the PNP-pincer ligand which led to a further increase in catalytic activity

(63 NH_3/Mo, respectively) [18]. In 2013, Peters et al. demonstrated that a catalytic synthesis of ammonia from N_2 is also possible based on iron complexes [19]. Using KC_8 and $HBAr^F$ at low temperature, up to 64 eq. NH_3 are generated per Fe center [12].

The earliest complete mechanistic scenario for synthetic nitrogen fixation is the Chatt cycle. This reactive scheme is based on mononuclear bis(dinitrogen) phosphine-Mo/W dinitrogen complexes supported by diphosphine ligands like dppe (dppe = $Ph_2PCH_2CH_2PPh_2$) or depe (depe = $Et_2PCH_2CH_2PEt_2$), which first have been synthesized by the groups of Chatt and Hidai [20–24]. Our group has been involved in synthetic, spectroscopic, and theoretical investigations of these complexes and their protonated/reduced derivatives over the last years [25–37]. The classic Chatt cycle, however, suffers from a couple of drawbacks that have limited its performance in a catalytic reaction mode. In particular, the conjugate base of the acid applied for protonation displaces one of the dinitrogen ligands in the parent bis (dinitrogen) complex, leading to a loss of 50% of bound substrate. Moreover, the presence of anionic coligands causes disproportionation at the Mo(I) stage which corresponds to 50% loss of reactive complex [38].

Herein we describe our attempts to modify the design of the original mononuclear Mo(0) phosphine complexes in order to eventually achieve a catalytic action of these systems. This in particular involves shielding the *trans*-position of coordinated N_2 in order to prevent ligand-exchange reactions at this site. The last stage of these developments is a molybdenum(0)–N_2 complex supported by a pentadentate tetrapodal (pentaPod) ligand. The N_xH_y ($x = 1, 2$; $y = 0$–3) intermediates in these types of systems should be related to those of the Schrock cycle and the Fe-based systems of Peters, but differ from those of Nishibayashi's system which does involve ligand-exchange reactions at the *trans*-position of coordinated N_2.

2 Mo(0)–Dinitrogen Complexes Supported by Tridentate PEP Ligands (E = P, N)

A first approach to occupy the *trans*-position of the coordinated dinitrogen ligand involved the use of tridentate PEP ligands. With the diphosphine coligand dmpm (dmpm = $Me_2PCH_2PMe_2$), we synthesized dinitrogen pentaphosphine complexes of the type [Mo(N_2)(PEP)(dmpm)] in which the *trans*-position of N_2 is occupied by the central donor atom E (E = P or N) of the tridentate ligand PEP. In 1988, George et al. had already prepared the mono(dinitrogen) complex [Mo(N_2)(dpepp)(dmpm)] supported by the tridentate ligand dpepp (dpepp = $PhP(CH_2CH_2PPh_2)_2$) [39]. The authors were also able to generate the corresponding NNH_2 complex by protonation with trifluoromethane sulfonic acid [40]. It should be mentioned that a range of molybdenum bis(dinitrogen) complexes with PEP ligands have been described in the literature [41–45], but – apart from [Mo(N_2)(dpepp)(dmpm)] and the related complex [Mo(N_2)(dpepp)(dppm)] (**1**) – no other molybdenum mono(dinitrogen) complexes with facially coordinating PEP ligands (E = P, N) were described. It was possible to obtain single crystals of **1** suitable for single crystal X-ray structure

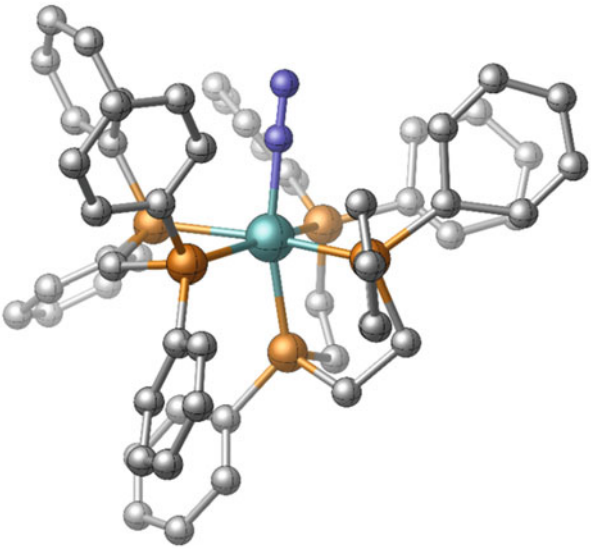

Fig. 1 Single crystal X-ray structure of [Mo(N_2)(dpepp)(dppm)] (**1**). Hydrogen atoms are omitted for clarity [41]

analysis (Fig. 1; [41]) demonstrating that the dpepp ligand coordinates facially to the molybdenum center.

In order to further explore such systems, we decided to investigate molybdenum–dinitrogen complexes with tridentate PEP ligands, varying the central donor atom E (E = N, P) and the chain length of the aliphatic linkages. Our goal was thereby to examine the stability of the respective N_2 complexes and the activation of the N_2 ligand [46]. A similar problem will be addressed when comparing the literature-known NP_3 ligand [47] (NP_3 = $N(CH_2CH_2PPh_2)_3$) with the new $prNP_3$ ($prNP_3$ = $N(CH_2CH_2CH_2PPh_2)_3$) ligand which has C_3 bridges (cf. Sect. 6) [48].

Elongation of the C_2 linkage of the tridentate ligand dpepp by an additional methylene group leads to the literature-known ligand prPP(Ph)P (prPP(Ph)P = PhP$(CH_2CH_2CH_2PPh_2)_2$) [49, 50]. In 1986, Dahlenburg et al. synthesized the corresponding molybdenum(III) complex [$MoCl_3$(prPP(Ph)P)]·CH_2Cl_2 which was converted to the bis(dinitrogen) complex [$Mo(N_2)_2$(prPP(Ph)P)(PR_3)] by sodium amalgam reduction using different monotertiary phosphines (PR_3) [50]. To the best of our knowledge, however, a corresponding molybdenum mono(dinitrogen) complex has not been synthesized yet. By sodium amalgam reduction of [$MoCl_3$(prPP(Ph)P)]·CH_2Cl_2 under a dinitrogen atmosphere in tetrahydrofuran in the presence of dmpm, we obtained the complex [Mo(N_2)(prPP(Ph)P)(dmpm)] (**2**) (Scheme 1) [46].

An X-ray single crystal structure determination of **2** has been performed (Fig. 2) [46]. Comparison with [Mo(N_2)(dpepp)(dppm)] **1** (Fig. 1) reveals similar bond lengths and angles (note that no crystal structure of [Mo(N_2)(dpepp)(dmpm)] is available).

Nevertheless, the Mo–P_{ax} bond of [Mo(N_2)(dpepp)(dppm)] **1** is about 0.0246(18) Å shorter than in **2** (2.4460(6) Å) [41, 46]. This significant difference is certainly due to higher steric demand of the C_3 bridges compared to the C_2 counterparts [46].

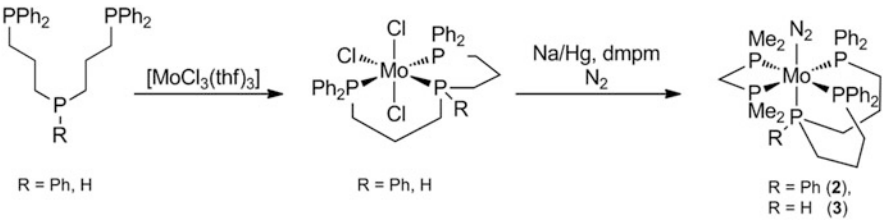

Scheme 1 Synthesis of the complexes [Mo(N_2)(prPP(Ph)P)(dmpm)] (**2**) and [Mo(N_2)(prPPHP)(dmpm)] (**3**)

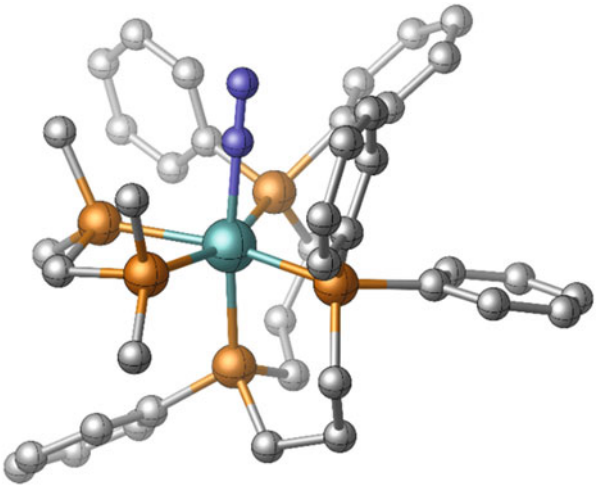

Fig. 2 Single crystal X-ray structure of [Mo(N_2)(prPP(Ph)P)(dmpm)] (**2**). Hydrogen atoms are omitted for clarity [46]

The degree of activation of the N_2 ligand can be investigated with the help of vibrational spectroscopy. Interestingly, replacement of the C_2 by a C_3 linkage hardly influences the N–N stretching frequency. For [Mo(N_2)(dpepp)(dmpm)] $\tilde{\nu}_{NN}$ is located at 1,966 cm^{-1} [39], and for [Mo(N_2)(prPP(Ph)P)(dmpm)] (**2**) a strong NN stretching vibration is observed at $\tilde{\nu}_{NN} = 1{,}970\ cm^{-1}$. Because of broadened signals and a quintet associated with the *trans*-phosphine in the ^{31}P-NMR spectrum of [Mo(N_2)(prPP(Ph)P)(dmpm)] (**2**), we assume that several conformers exist in solution. The corresponding complex [Mo(N_2)(dpepp)(dppm)] (**1**) shows a triplet for the *trans*-phosphine instead of a quintet. The presence of several conformers of **2** can be explained by the higher flexibility of the C_3 linkages as compared to the C_2 bridges of dpepp in [Mo(N_2)(dpepp)(dmpm)] [39].

In view of the fact that the flexibility of the ligand backbone is restricted by phenyl groups [51], we wanted to know what happens if the tertiary phosphine *trans* to the N_2 ligand is replaced by a secondary phosphine. Therefore we synthesized the complex [Mo(N_2)(prPPHP)(dmpm)] (**3**) with the ligand prPPHP (prPPHP = HP($CH_2CH_2CH_2PPh_2$)$_2$) (Scheme 2). The synthesis of the diallylphosphonic acid ethyl ester was adapted from Bujard et al. [52]. After addition of diphenylphosphine,

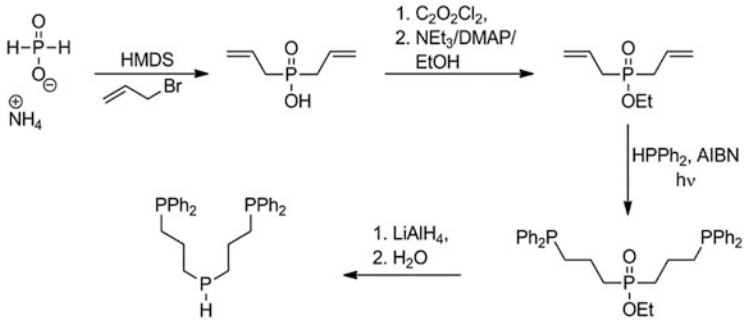

Scheme 2 Synthesis of the ligand prPPHP

promoted by AIBN, we obtained ethyl-bis(3-(diphenylphosphino)propyl)phosphinate, which was subjected to a lithium aluminium hydride reduction, leading to the ligand prPPHP [46].

By amalgam reduction of the Mo(III) precursor, the Mo(0)–N_2 complex [Mo(N_2)(prPPHP)(dmpm)] (**3**) was obtained. Again the ^{31}P-NMR spectrum indicates the presence of several conformers. Moreover a strongly high-field shifted signal for the *trans* secondary phosphine is observed [46]. A single crystal structure of **3** shows similar bond lengths and angles as compared to **2**. However, with 2.4015(6) Å the Mo–P_{ax} bond is significantly shorter than those present in [Mo(N_2)(prPP(Ph)P)(dmpm)] (**2**) (2.4460(6) Å) [46] and [Mo(N_2)(dpepp)(dppm)] (2.4214(18) Å) [41]. This is readily explained by the smaller steric demand of the PH group as compared to the PPh moiety [46]. Interestingly the NN stretching band of **3** ($\tilde{\nu}_{NN}$ = 1,974 cm^{-1}) is nearly the same as in **2** ($\tilde{\nu}_{NN}$ = 1,970 cm^{-1}) so that the activation of N_2 is not influenced by replacing the PPh moiety by PH [46].

The effect of changing the central donor atom of the PEP ligand was investigated by replacing the central phosphorus donors of dpepp and prPP(Ph)P by nitrogen, leading to the ligands PN(Ph)P (PN(Ph)P = PhN($CH_2CH_2PPh_2$)$_2$) and prPN(Ph)P (prPN(Ph)P = PhN($CH_2CH_2CH_2PPh_2$)$_2$). The former ligand has been prepared earlier by Kostas [53]. The ligand PN(Ph)P was converted to Mo(III) complexes [MoX_3(PN(Ph)P)] using the Mo(III) precursors [$MoCl_3$(thf)$_3$], [$MoBr_3$(thf)$_3$], and [MoI_3(thf)$_3$] (Scheme 3) [54–56]. The highest yield was achieved with the precursor [MoI_3(thf)$_3$] [46]. Interestingly ligand prPN(Ph)P could only be converted to the Mo(III) complex with [MoI_3(thf)$_3$] [46].

Reduction of the Mo(III) complexes with sodium amalgam under a dinitrogen atmosphere predominantly leads to the mono(dinitrogen) complex [Mo(N_2)(PN(Ph)P)(dmpm)] (**4**) and the bis(dinitrogen) complex [Mo(N_2)$_2$(κ^2-PN(Ph)P)(dmpm)] (**5**; Scheme 3) [46]. A similar pathway has been employed to synthesize the corresponding prPN(Ph)P complexes [Mo(N_2)(prPN(Ph)P)(dmpm)] (**6**) and the [Mo(N_2)$_2$(κ^2-prPN(Ph)P)(dmpm)] (**7**). The occurrence of the bis(dinitrogen) complexes in both systems indicates a partial dissociation of the N-donor in *trans*-position of the N_2 ligand. Thereby a κ^2-coordination of the prPN(Ph)P ligand results and another N_2

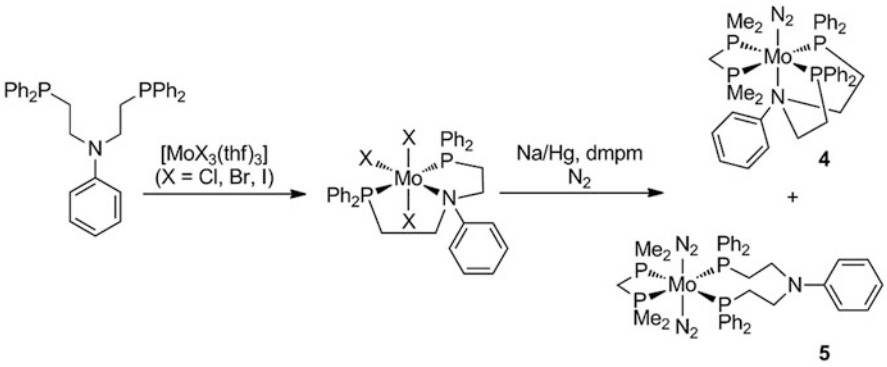

Scheme 3 Synthesis of the complexes [MoX_3(PN(Ph)P)] (X = Cl, Br, I), [Mo(N_2)(PN(Ph)P)(dmpm)] (**4**), and [Mo(N_2)$_2$(PN(Ph)P)(dmpm)] (**5**)

ligand coordinates at the free position (Scheme 3). Note that the smallest fraction of the respective bis(dinitrogen) complex was observed if [MoI_3(PN(Ph)P)] was used as a precursor [46].

The NN stretching vibration of [Mo(N_2)(PN(Ph)P)(dmpm)] (**4**) is observed at 1,940 cm^{-1} and that of [Mo(N_2)(prPN(Ph)P)(dmpm)] (**6**) at 1,939 cm^{-1}. This demonstrates again that an elongation of the C_2 to a C_3 linkage does not influence the N_2 activation (vide infra). Comparing the NN stretch of [Mo(N_2)(PN(Ph)P)(dmpm)] (**4**) with that of the phosphorus analogue [Mo(N_2)(dpepp)(dmpm)] ($\tilde{\nu}_{NN} = 1{,}966\ cm^{-1}$), a low-frequency shift of 26 cm^{-1} is observed. Exchange of a phosphine by an amine in *trans*-position to the N_2 ligand thus drastically increases the activation of N_2. Supported by DFT calculations, we assume that the absence of a π-backbonding interaction in the PNP system ensures a better activation. By contrast, a P-donor *trans* to the N_2 ligand shows significant π-backbonding, leading to a stronger bond between the metal and the *trans* P-donor which reduces the activation of N_2 [46].

Summing up, the elongation of a C_2 to a C_3 linkage and the exchange of tertiary phosphine by a secondary phosphine hardly influence the activation of N_2 but an N-donor *trans* to N_2 leads to a better activation of N_2. On the other hand, mono (dinitrogen) complexes with PNP ligands are less stable than their PPP counterpart ligands so that bis(dinitrogen) complexes are formed [46].

3 Mo(0)–Dinitrogen Complexes Supported by Mixed Imidazol-Ylidene/Phosphanyl Hybrid Ligands

Since the isolation of the first stable N-heterocyclic carbene by Arduengo and coworkers in 1991 [57, 58], these molecules have become increasingly important, particularly in organometallic catalysis [59–63]. For that reason, it appeared of significant interest to explore the application of mixed phosphine/carbene ligands in the field of small

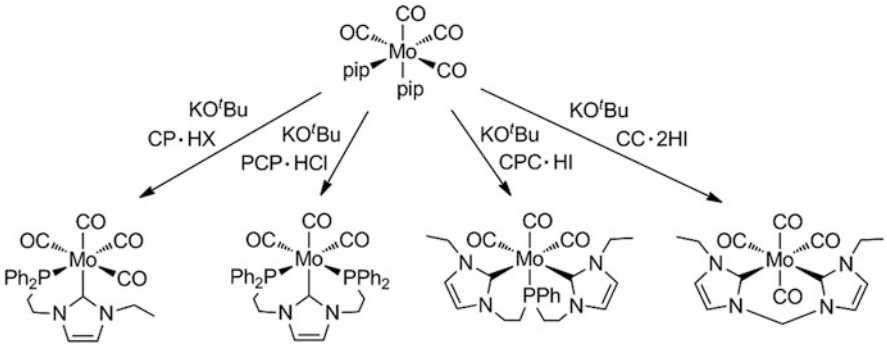

Scheme 4 Different molybdenum complexes have been prepared starting from the precursor [Mo $(CO)_4(pip)_2$]

molecule activation, especially molybdenum-based dinitrogen fixation [64–66]. In our studies of molybdenum–dinitrogen complexes supported by multidentate phosphine ligands, we investigated the electronic influences of aryl and alkyl substituents in detail [46, 67–71]. Far more drastic changes are to be expected if a phosphine group is replaced by a carbene residue [64]. To determine the impact of N-heterocyclic carbenes coordinating to a molybdenum center on the activation of small molecules, Gradert et al. synthesized a range of molybdenum tricarbonyl complexes supported by different carbene and mixed carbene/phosphine ligands. Starting from the precursor [Mo $(CO)_4(pip)_2$] and replacing the piperidine ligands (and one carbonyl ligand), four new complexes have been obtained (Scheme 4). Using vibrational spectroscopy and single crystal X-ray structure analysis, these complexes have been characterized. Furthermore DFT calculations have been performed to determine the electronic properties of the carbene unit [64].

As evident from Scheme 4, the bidentate CP ligand and the CC ligand coordinate to the molybdenum center via the phosphine and carbene unit or the pure carbene groups, respectively. The PCP ligand and the CPC ligand substitute the two piperidine ligands and one CO ligand of the precursor $[Mo(CO)_4(pip)_2]$.

In almost all cases, potassium *tert*-butoxide was used as deprotonating agent. The free carbene reacts with the metal precursor in tetrahydrofuran to yield the molybdenum complexes $[Mo(CO)_4(CP)]$, $[Mo(CO)_3(PCP)]$, $[Mo(CO)_3(CPC)]$, and $[Mo(CO)_4(CC)]$ supported by mixed NHC/phosphine ligands. It could be shown that the $[Mo(CO)_4(pip)_2]$ precursor with its internal base piperidine is able to act as the deprotonating agent. Consequently the use of an external base was not required. The molybdenum triscarbonyl complexes containing the PCP or CPC ligand have been investigated using vibrational spectroscopy, nuclear magnetic resonance spectroscopy, and single crystal X-ray structure analysis. Importantly, the tridentate ligand PCP coordinates facially to the molybdenum center (Fig. 3); the same is observed for the CPC ligand [64].

Relevant information regarding the properties of the metal–carbene bond could be obtained from single crystal X-ray structure determination. Comparing the

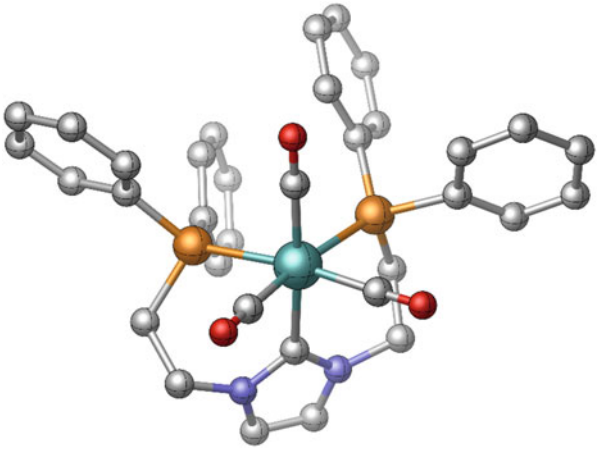

Fig. 3 Crystal structure of *fac*-[Mo(CO)$_3$(PCP)]. Hydrogen atoms are omitted for clarity [64]

impact of the carbene unit on the carbonyl ligand in *trans*-position with the influence of a phosphine group in *trans*-position to a carbonyl ligand, it became clear that the C–O bond distance of the carbonyl ligand *trans* to the carbene (1.158 Å) is longer than the C–O distances of the CO ligands *trans* to the phosphines (1.149 Å/1.150 Å). This was interpreted as evidence that carbene is a weaker π-acceptor than phosphine. To assess the σ-donor capabilities of the different donor atoms of the PCP ligand, the metal–$C_{Carbonyl}$ bond distances of the three CO ligands were compared. The metal–$C_{Carbonyl}$ distance of the CO *trans* to the carbene (1.969 Å) is marginally shorter than the distances of the CO ligands *trans* to the phosphine moieties (1.978 Å/1.972 Å). Because of the missing elongation of the metal–C_{CO} bond *trans* to the carbene unit, the σ-donor capability of the carbene has to be comparable to that of the phosphine [64].

To check these conclusions, DFT calculations have been performed. Between the lone pair of the carbene and the metal dσ orbital, a distinct, strong σ-interaction exists. Furthermore a π-interaction between the $C_{carbene}$ atom and the metal center is conceivable. Depending on the nature of the metal center (number of d electrons), the π-contribution varies between 10 and 30% [72]. In a molybdenum(0) center, the d_{xy}, d_{yz}, and d_{xz} orbitals are doubly occupied so that the lone pair of the carbene donates into the $d_{x^2-y^2}$ ([Mo(CO)$_4$(CP)] and [Mo(CO)$_4$(CC)]) and d_{z^2} ([Mo(CO)$_3$(PCP)], [Mo(CO)$_3$(CPC)]) orbitals, respectively. Comparing the different contributions of the carbene and phosphine lone pairs, it is obvious that the σ-donor capability of these groups is of about equal strength. This is illustrated by the isodensity plots of the frontier orbitals shown in Fig. 4.

Regarding the carbene moiety in Fig. 4, it becomes clear that there is no π-interaction (neither π-bonding nor π-backbonding) between the dπ orbitals of the metal center and the carbene C atom. DFT thus indicates that the carbene unit of the PCP ligand coordinating to a Mo(0) center is only a strong σ-donor, but not a π-acceptor [64].

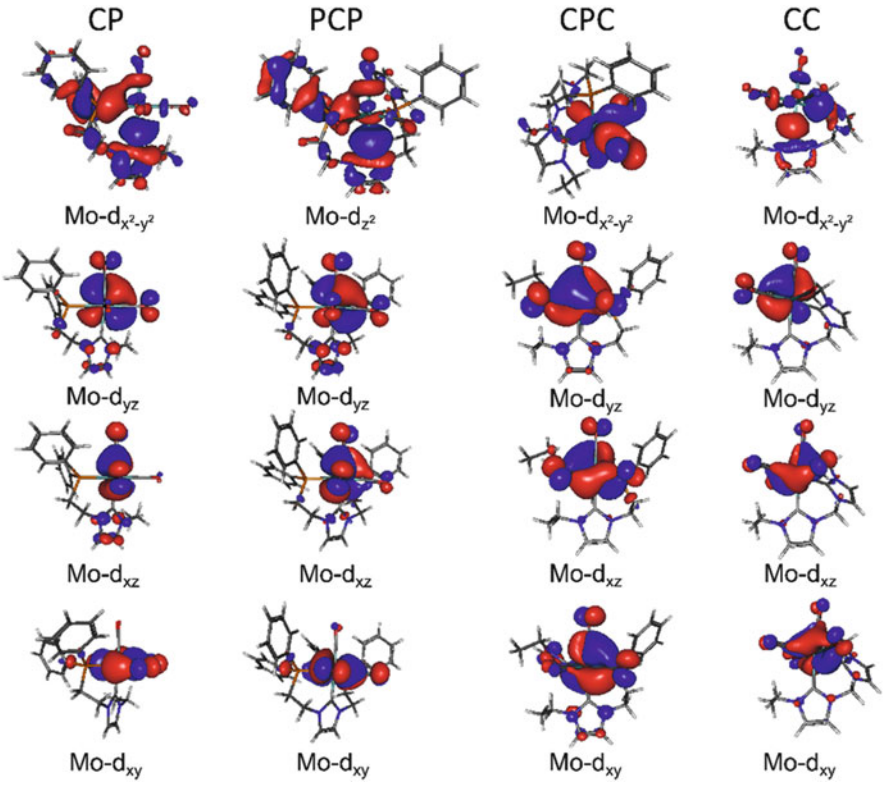

Fig. 4 Isodensity plots of the frontier molecular orbitals of $[Mo(CO)_4(CP)]$, $[Mo(CO)_3(PCP)]$, $[Mo(CO)_3(CPC)]$, and $[Mo(CO)_4(CC)]$. The σ-donor capability of the phosphine and carbene unit is of comparable strength [64]

The results of vibrational spectroscopy support these findings. The bond length between two atoms correlates with the vibrational frequency; that is, the longer the bond, the lower the frequency. In order to obtain information regarding this issue, seven complexes with phosphine, carbene, and mixed phosphine/carbene donor sets have been synthesized and investigated with IR and Raman spectroscopy (Scheme 5). Four complexes are tetracarbonyl complexes containing bidentate coligands, whereas three complexes are tricarbonyl complexes supported by tridentate coligands. Complexes $[Mo(CO)_4(CC)]$ and $[Mo(CO)_4(dppp)]$ (dppp = $Ph_2PCH_2CH_2CH_2PPh_2$) exhibit C_{2v} symmetry; hence four bands (2^*A_1, B_1, and B_2) appear in the vibrational spectrum. Due to the mixed ligand sphere, the point group of $[Mo(CO)_4(CP)]$ is lowered to C_s, and as a result the four observable bands transform according to $2^*A'$ and $2^*A''$ [64].

The frequency of the totally symmetric mode A_1/A' in the complexes with PP, CP, and CC ligands decreases from 2,016 cm^{-1} (PP) over 2,005 cm^{-1} (CP) to 1,987 cm^{-1} (CC). This indicates that carbonyl ligands are more activated in carbene complexes than in complexes with pure phosphine ligands. The same behavior can be observed

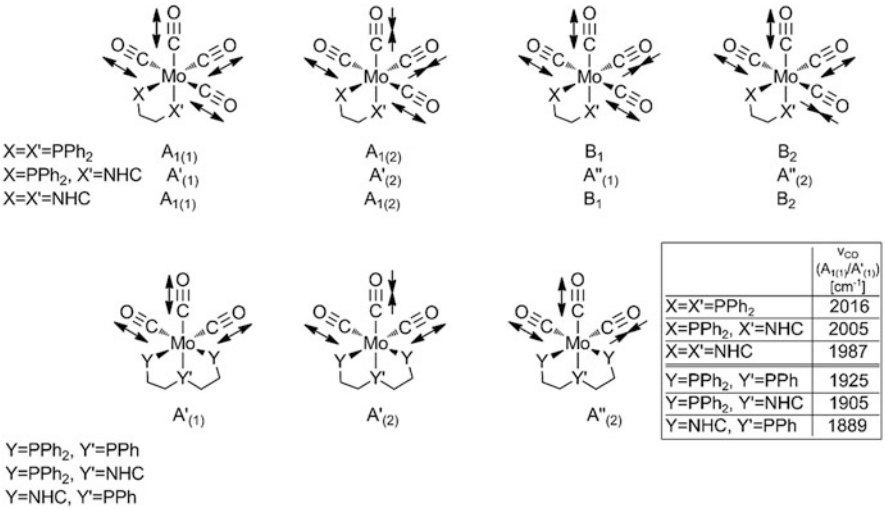

	ν_{CO} ($A_{1(1)}/A'_{(1)}$) [cm^{-1}]
X=X'=PPh$_2$	2016
X=PPh$_2$, X'=NHC	2005
X=X'=NHC	1987
Y=PPh$_2$, Y'=PPh	1925
Y=PPh$_2$, Y'=NHC	1905
Y=NHC, Y'=PPh	1889

Scheme 5 Analysis of the vibrational modes depending on the symmetry of the complexes

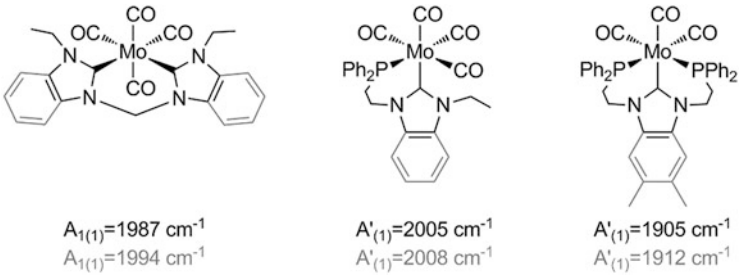

Scheme 6 New synthesized molybdenum complexes bearing benzimidazole-based mixed NHC/phosphine ligands

in the complexes with tridentate ligands. Three bands are observed in the IR and Raman spectra of [Mo(CO)$_3$(CPC)], [Mo(CO)$_3$(PCP)], and [Mo(CO)$_3$(dpepp)] which in C_s symmetry transform according to 2*A′ and A″ [73]. The stretching vibration of [Mo(CO)$_3$(CPC)] is located at 1,889 cm^{-1}, the vibration of [Mo(CO)$_3$(PCP)] at 1,905 cm^{-1}, and the totally symmetric mode of [Mo(CO)$_3$(dpepp)] is located at 1,925 cm^{-1} [64]; that is, the more carbene units are coordinated to the metal center, the lower are the CO frequencies.

In a later study, Gradert et al. synthesized similar molybdenum carbonyl complexes with mixed N-heterocyclic/phosphine ligands. The effect of a carbene unit with a benzimidazole backbone towards small molecules like CO was also investigated and compared to the imidazole-based carbene moiety. In Scheme 6, the new complexes [Mo(CO)$_4$(Benz-CC)], [Mo(CO)$_4$(Benz-CP)], and [Mo(CO)$_4$(DMBenz-PCP)] are shown [65, 74].

Vibrational studies showed that the benzimidazole-based ligands have comparable properties to the imidazole-based counterparts. However, the CO stretching vibrations of the molybdenum complexes coordinated by the carbene ligand with benzimidazole backbones are slightly shifted to higher wavenumbers (Scheme 6). In comparison to the $[Mo(CO)_4(CC)]$ complex, e.g., the stretching frequency of the benzimidazole analogue $[Mo(CO)_4(Benz\text{-}CC)]$ is shifted by 7 cm^{-1} to 1994 cm^{-1}. The same effect can be observed in the complexes with tridentate ligands, where the totally symmetric stretching mode in the benzimidazole-based NHC/phosphine CO complex is shifted by 7 cm^{-1} to higher frequency compared to the imidazole-based analogue [64, 65]. Two explanations can be invoked to explain these findings: (1) The carbene unit of the benzimidazole-based ligand is a weaker σ-donor than the carbene of the imidazole-based ligand. (2) The σ-donor capabilities of both ligand systems are comparable and the benzimidazole-based carbene ligand also functions as a π-acceptor. To evaluate these possibilities, DFT calculations were performed. As evident from Fig. 5, the isodensity plots of the uncoordinated benzimidazole ligand exhibit an unoccupied π* orbital which is located at the carbene atom (LUMO, −0.59 eV) [65]. Backbonding to this orbital could in principle be possible. Although the DFT-optimized and the X-ray structure exhibit a slightly shortened Mo–C_{NHC} bond for $[Mo(CO)_3(DMBenz\text{-}PCP)]$, no significant contribution of π* orbitals is found in the dπ orbitals of the molybdenum atom of the complex. Consequently the lower activation of the carbonyl ligand in the

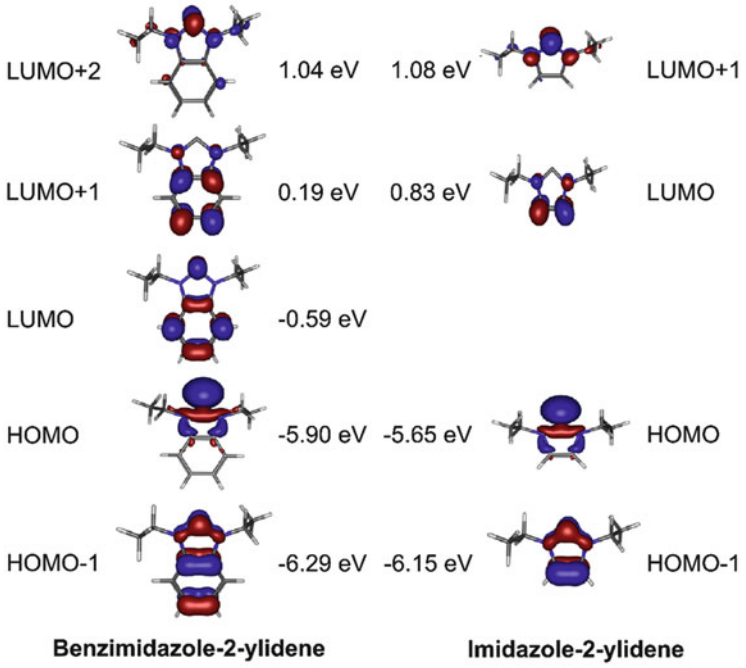

Fig. 5 Isodensity plots of the frontier molecular orbitals of the imidazole and benzimidazole-based PCP ligands and the energies [65]

benzimidazole–PCP moiety is caused by a lower σ-donor capability of the carbene moiety as compared to the imidazole-based system [65].

In conclusion, the first molybdenum carbonyl complexes supported by mixed phosphine/NHC ligands have been prepared and characterized by different methods. In agreement with single crystal X-ray structure determination and vibrational spectroscopy, DFT calculations indicate that the carbene unit within the ligand systems is a pure σ-donor, in contrast to a phosphine moiety which is a σ-donor/π-acceptor. Due to the missing π-acceptor properties, the carbonyl ligands in the carbene complexes are significantly more activated than those in complexes with pure phosphine coligands [64]. Additionally three carbonyl complexes containing mixed benzimidazole-based NHC/phosphine ligands have been prepared, characterized, and compared to their imidazole analogues. The benzimidazole-based ligand is a weaker σ-donor than the imidazole-based ligand and, therefore, the CO ligands are slightly less activated in molybdenum carbonyl complexes supported by benzimidazole- as compared to imidazole-based ligands [65].

Having analyzed the bonding properties of NHC ligands based on molybdenum carbonyl complexes, the next step involved the application of the mixed NHC/phosphine ligands in molybdenum-based nitrogen fixation [66]. The tridentate mixed NHC/phosphine ligand 1,3-bis(2-diphenylphosphanylethyl)imidazol-2-ylidene (PCP) was chosen for the synthesis of molybdenum–dinitrogen complexes. Starting from the precursor $[Mo(N_2)_2(PPh_2Me)_4]$, ligand-exchange reactions were explored to synthesize mono(dinitrogen) complexes containing the PCP ligand or to *synthesize* other suitable precursors (Scheme 7) [66, 75–77]. The four monophosphine ligands in the complex $[Mo(N_2)(PPh_2Me)_4]$ can easily be substituted by two diphosphine ligands or two phosphite ligands. The resulting molybdenum–dinitrogen complexes have been investigated using NMR and vibrational spectroscopy. Depending on the dppm, dmpm, or two trimethyl phosphite ligands, the dinitrogen moieties are more or less activated. The symmetric stretching mode is located at 2,034 cm^{-1} ($[Mo(N_2)_2(dppm)(PPh_2Me)_2]$ (**8**)), at 2,004 cm^{-1} ($[Mo(N_2)_2(dmpm)(PPh_2Me)_2]$ (**9**)), and at 2,048 cm^{-1} ($[Mo(N_2)_2(PPh_2Me)_2(P(OMe)_3)_2]$ (**10**)). The typical AA′XX′ coupling pattern can be observed for the two complexes with pure phosphine ligands $[Mo(N_2)_2(dppm)(PPh_2Me)_2]$ (**8**) and $[Mo(N_2)_2(dmpm)(PPh_2Me)_2]$ (**9**) [66].

Starting from $[Mo(N_2)_2(PPh_2Me)_4]$, the ligand-exchange reaction with the PCP ligand has been monitored using IR spectroscopy. Within 2 h, the symmetric and antisymmetric stretching modes of the bis(dinitrogen) precursors disappear and a new band emerges at 1,876 cm^{-1} (Fig. 6) [66].

Due to the very strong activation of the N_2 ligand and the results of the investigations of the molybdenum carbonyl complexes supported by the PCP ligand, it can be assumed that the dinitrogen ligand coordinates in *trans*-position to the carbene atom. Because of the flexibility of the PCP ligand and steric hindrance of the phenyl groups, the constitution corresponds to the meridionally coordinated complex *mer*-$[Mo(N_2)(PCP)(PPh_2Me)_2]$ (**11**). However, the strong activation of the N_2 ligand is accompanied by a high thermal instability of the dinitrogen complex, and therefore further investigations using NMR spectroscopy could not be performed. Reaction of the precursor $[Mo(N_2)_2(dppm)(PPh_2Me)_2]$ (**8**) with the carbene ligand did not lead

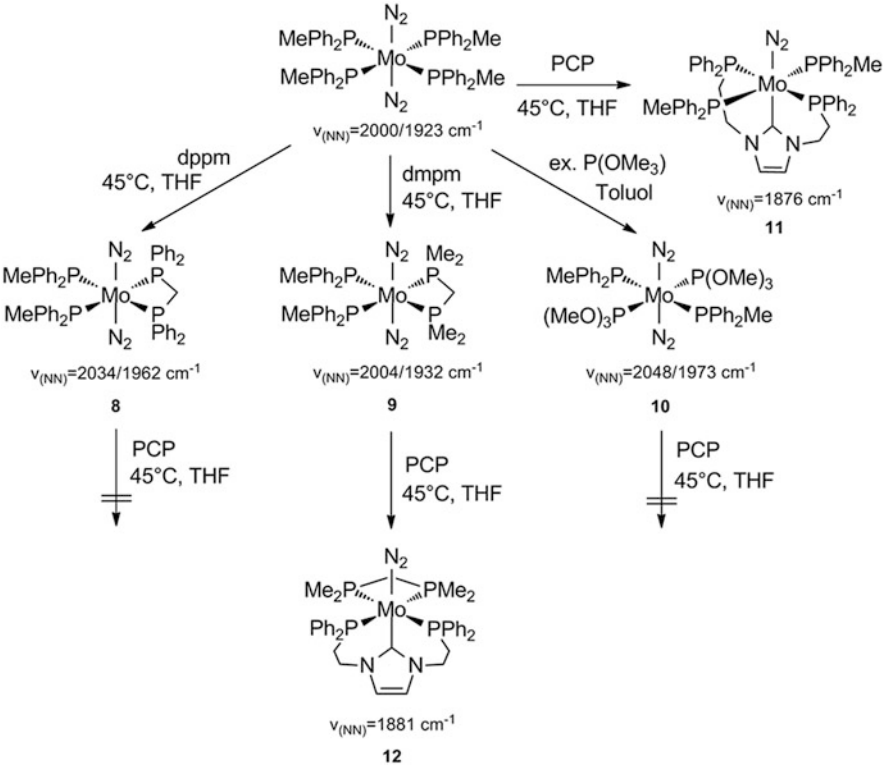

Scheme 7 Dinitrogen complexes with different phosphine and phosphite ligands

to the expected N_2 complex. A possible reason is the high steric demand of the phenyl groups of the dppm ligand. The PCP ligand has to coordinate facially to the molybdenum center, so that the four phenyl groups in the horizontal plane interfere excessively. The analogous complex with the dmpm coligand could be obtained, exhibiting an NN stretching vibration at 1,881 cm^{-1}. Time-dependent NMR spectroscopy revealed the formation of the *fac*-[$Mo(N_2)$(dmpm)(PCP)] (**12**) complex during the reaction. Nevertheless, due to the strong activation of the dinitrogen ligand, the product also was thermally unstable. The strong activation of the N_2 ligand and the thermal instability of the complex are caused by the pure σ-donor and the missing π-acceptor character of the PCP ligand. In order to obtain dinitrogen complexes which exhibit a higher thermal stability, the PCP ligand was substituted by the DMBenzPCP ligand [74]. However, the desired complexes could not be isolated [66].

In view of these results, we decided to replace the phosphine coligands by less activating trimethyl phosphite ligands. This way the electron density at the molybdenum center should be reduced so that the coordinating N_2 ligand is less activated and the corresponding complex is stable at room temperature. First of all a ligand-exchange reaction starting from [$Mo(N_2)_2(PPh_2Me)_2(P(OMe)_3)_2$] (**10**) with the PCP

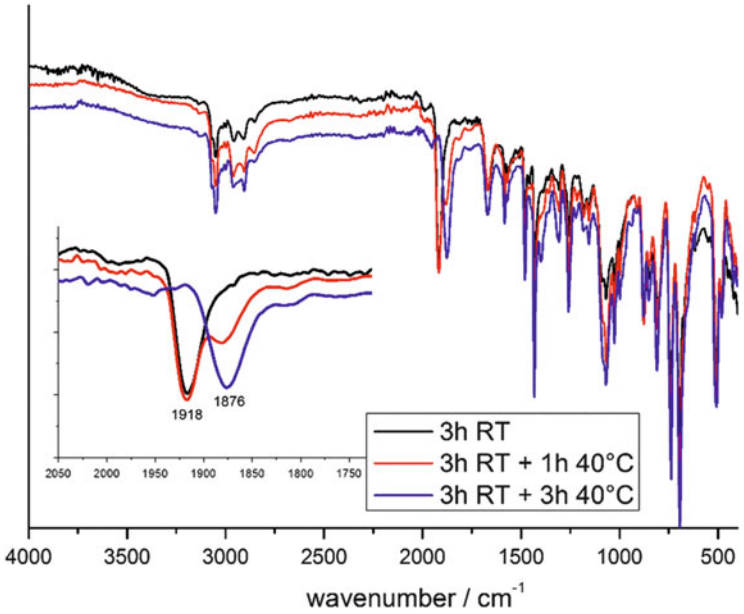

Fig. 6 IR spectra of the reaction of $[Mo(N_2)_2(PPh_2Me)_4]$ and the PCP ligand [66]

ligand has been performed. The structure of the precursor $[Mo(N_2)_2(PPh_2Me)_2(P(OMe)_3)_2]$ (**10**) was proven by single X-ray structure analysis in the solid state and by NMR spectroscopy in solution. In the solid state, the pure *trans–trans* isomer exists, where the two phosphines as well as the two phosphites are in *trans*-position to each other. In solution, this complex converts into several isomers. Hence the ligand-exchange reaction of this precursor with the PCP ligand does not yield the dinitrogen complex.

A further possibility to obtain molybdenum(0)–dinitrogen complexes is the reduction of a molybdenum(III) complex by use of, e.g., sodium amalgam. The single crystal X-ray structure determination of the precursor $[MoCl_3(PCP)]$ proves a meridional coordination of the PCP ligand. Comparing this coordination geometry to that of the molybdenum triscarbonyl complexes (vide supra), it becomes clear that the coordination mode of the PCP ligand depends on the electronic properties of the coligand (chloride vs. carbonyl) [66]. Sodium amalgam reduction of the molybdenum(III) precursor $[MoCl_3(PCP)]$ under N_2 atmosphere in the presence of two equivalents of trimethyl phosphite finally led to two molybdenum(0) complexes **13** and **14** (Scheme 8).

The target complex *mer*-$[Mo(N_2)(PCP)(P(OMe)_3)_2]$ (**13**) could be obtained this way and was found to be thermally stable. In accordance to our expectations, the NN stretching vibration of this dinitrogen complex is located at higher wavenumbers at 1,932 cm^{-1}. The decrease in the activation of the dinitrogen ligand leads to a stable product which could be characterized completely. DFT calculations of the complex *mer*-$[Mo(N_2)(PCP)(P(OMe)_3)_2]$ (**13**) exhibit no π-backbonding into π* orbitals of

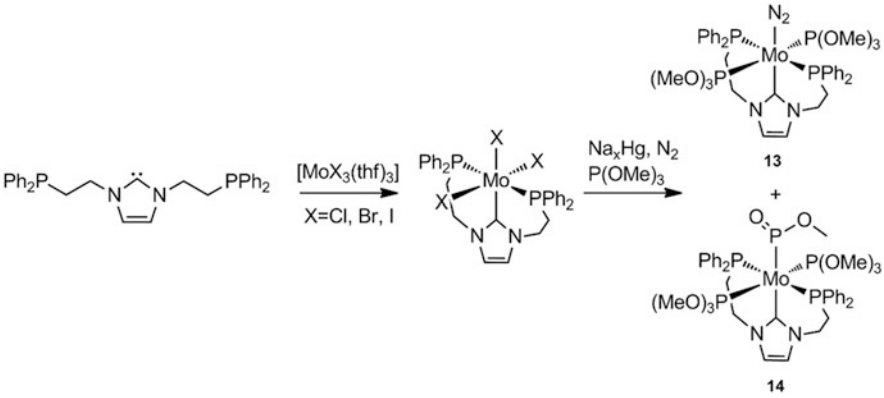

Scheme 8 Reaction of the free carbene with the molybdenum precursor $[MoCl_3(thf)_3]$ and the sodium amalgam reduction under N_2 atmosphere and two equivalents of trimethyl phosphite

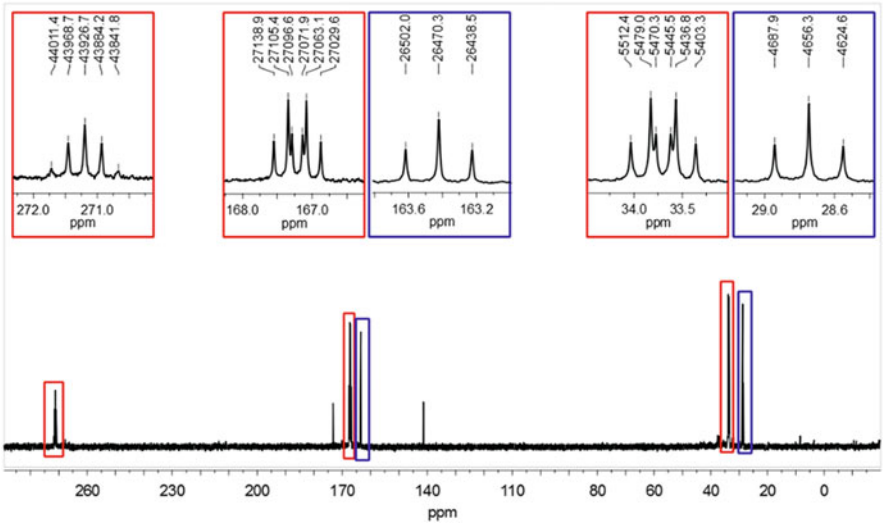

Fig. 7 ^{31}P-NMR spectrum of *mer*-$[Mo(N_2)(PCP)(P(OMe)_3)_2]$ (**13**) (*blue*) and $[Mo(PCP)(P(OMe)_3)_2(P(O)(OMe))]$ (**14**) (*red*) [66]

the PCP ligand. Again, the carbene atom of the PCP ligand is a pure σ-donor. Regarding the ^{31}P-NMR spectrum of the product of the sodium amalgam reduction, it is apparent that an additional product has been formed. Because of the signal in the ^{13}C HMBC NMR spectrum at 193.8 ppm, the coordination of the carbene atom to the molybdenum center in this additional product is proven. In the ^{31}P-NMR spectrum, the expected two triplets of the dinitrogen complex can be observed (Fig. 7) [66].

Furthermore three additional signals of the other product are visible. A multiplet at 271.0 ppm points towards a new phosphorus species coordinated to the molybdenum center. This strong shift is not compatible with the trimethyl phosphite or phosphine groups. Ultimately, the structure of the by-product **14** could be solved by single X-ray structure determination. It is shown in Fig. 8 [66].

In *trans*-position to the carbene unit, the species P(O)(OMe) coordinates to the molybdenum center. The Mo-$P_{P(O)(OMe)}$ bond is significantly shortened (2.254(1) Å) compared to the other Mo–P bonds (2.397(8) Å and 2.453(8) Å). As a result of this, it can be inferred that the Mo–$P_{P(O)(OMe)}$ bond has a double-bond character. Vibrational spectroscopic analysis reveals a P-$O_{P(O)(OMe)}$ stretching vibration at 1,146 cm^{-1} which is indicative of a double bond. The ligand P(O)(OMe) can be described as an ester of meta phosphorous acid, so it can be denoted as a meta phosphite ligand [78–82]. By varying the amount of trimethyl phosphite, it is possible to change the ratio of the dinitrogen complex and the meta phosphite complex up to 3:2 (1.4 equiv. of trimethyl phosphite). However, it is not possible to suppress the formation of the meta phosphite complex completely. By further lowering the amount of trimethyl phosphite, the yield of the dinitrogen complex decreases but the ratio of the products is unchanged. Using an excess of trimethyl phosphite leads to the exclusive formation of the meta phosphite complex. These experiments show that the formation of the meta phosphite complex [Mo(PCP)$(P(OMe)_3)_2$(P(O)(OMe))] (**14**) is preferred; that is, this is the thermodynamically stable product [66].

The formation of this complex has been investigated in more detail. Using the ligand dpepp instead of PCP during the sodium amalgam reduction and applying an excess of trimethyl phosphite lead to the molybdenum complex *fac*-[Mo$(P(OMe)_3)_3$(dpepp)]. No formation of a meta phosphite complex is observed. Accordingly the reaction of trimethyl phosphite to a meta phosphite ligand is exclusively mediated by the Mo-NHC unit. During time-dependent NMR studies of the product mixture ([Mo(PCP)$(P(OMe)_3)_2$(P(O)(OMe))] (**14**) and *mer*-[Mo(N_2)(PCP)$(P(OMe)_3)_2$] (**13**)) in presence of an excess of trimethyl phosphite, the ratio of the starting products

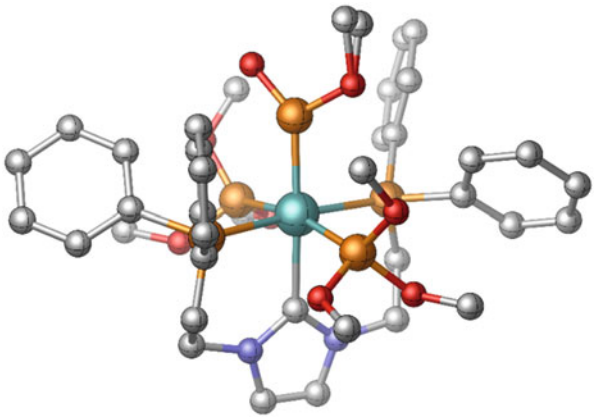

Fig. 8 Crystal structure of [Mo(PCP)$(P(OMe)_3)_2$(P(O)(OMe))] (**14**). Hydrogen atoms are omitted for clarity [66]

does not change. Thus the sodium amalgam reduction of a molybdenum(III) complex to a molybdenum(0) complex is needed to generate the meta phosphite [66].

The reactivity of the dinitrogen complex *mer*-[Mo(N_2)(PCP)($P(OMe)_3$)$_2$] (**13**) towards Brønsted and Lewis acids has been investigated in order to evaluate the influence of the NHC unit. Intermediates like NNH_2^- or $AlMe_3$ complexes could not be observed during the reaction using ^{31}P-NMR spectroscopy. Instead the meta phosphite complex reacts with the Lewis acid $AlMe_3$ under formation of two different products, in which the $AlMe_3$ coordinates to the two different oxygen atoms of the meta phosphite ligand [66].

To summarize, new molybdenum complexes containing the imidazole- and benzimidazole-based pincer ligand PCP (1,3-bis(2-diphenylphosphanylethyl) imidazol-2-ylidene, resp., 1,3-bis(2-diphenylphosphanylethyl)benzimidazol-2-ylidene) have been synthesized, characterized, and investigated in connection with small molecule, especially dinitrogen fixation [64–66]. It became apparent that the carbene atom of the PCP ligand is a pure σ-donor because of the exact cancellation of the π-donor and π-acceptor properties. Hence small molecules like carbonyl or dinitrogen coordinating to the metal center exhibit a very strong activation of the triple bond [64–66]. Unfortunately, this high activation of the dinitrogen ligand is accompanied by a thermal instability of the resulting complexes [66]. Therefore the electron density at the metal center has been reduced using phosphite ligands. A stable dinitrogen molybdenum complex with a mixed phosphine/carbene ligand could be obtained and characterized. During this reaction, the by-product [Mo(PCP)($P(OMe)_3$)$_2$(P(O)(OMe))] (**14**) with a meta phosphite ligand has emerged as the thermodynamically stable product. The derivatization of the dinitrogen complex *mer*-[Mo(N_2)(PCP)($P(OMe)_3$)$_2$] (**13**) only leads to a decomposition [66]. The study of the mixed ligands with phosphine and carbene units revealed the remarkable properties of the PCP ligand although the application in mononuclear molybdenum–dinitrogen complexes is delicate [64–66].

4 Mo(0)–Dinitrogen Complexes Supported by Tripodal Ligands with Aryl Substituents

In this section, we return to molybdenum–dinitrogen complexes supported by polydentate phosphine ligands. In Sect. 2, the use of linear tridentate PEP ligands was explored, varying the donor atom E (N, P) and the chain length of the phosphine arms (C_2 vs. C_3). A potential disadvantage especially of the dpepp system is the possibility of the existence of different facial isomers, leading to different degrees of N_2 activation [41, 83].

In order to establish a design that both remedies the drawbacks of the Chatt system and avoids the problem of isomerization, our working group explored the use of tripodal triphosphine ligands for molybdenum-based nitrogen fixation. In contrast to their linear PPP counterparts, especially the dpepp ligand, these ligands

enforce facial coordination [84]. In this way, the pivotal *trans*-position to the dinitrogen ligand is also saturated. Moreover, due to the chelating effect of the ligand, an increased stability at higher oxidation states of the metal center is expected. In this respect, tripodal triphosphine ligands represent an alternative to tridentate macrocyclic P3 ligands [85]. In 2011, we reported the first successful coordination of the tripod ligand tdppme (tdppme = 1,1,1-tris(diphenylphosphanylmethyl)ethane) to a low-valent Mo–dinitrogen complex along with the bidentate coligands dmpm and dppm, respectively [67]. The applied synthetic approach involved the reaction of strong reducing agents like sodium amalgam with Mo(III) halide complexes to generate – along with the respective coligands under a dinitrogen atmosphere – the corresponding molybdenum–dinitrogen complexes (vide supra). In the case of the tdppme ligand, the best results were achieved by starting from $[MoBr_3(thf)_3]$ (Scheme 9). Reaction with the tripod led to $[MoBr_3(tdppme)]$; notably that the *mer*-isomer of $[MoBr_3(thf)_3]$ changes to the *fac*-isomer of $[MoBr_3(tdppme)]$ in the course of the reaction. The sodium amalgam reduction under an N_2 atmosphere in the presence of the appropriate diphos coligand ultimately produced the complexes $[Mo(N_2)(tdppme)(diphos)]$ (**15**, **16**).

The constitution of these complexes in the solid state was elucidated by the single crystal X-ray structure analysis of the complex $[Mo(N_2)(tdppme)(dmpm)]$ (**16**) (Fig. 9). The data show a rather small bite angle of 66.86° of the dmpm coligand which seems to fit to the higher steric demand of the tripod ligand exhibiting a larger bite angle of the equatorial phosphines (82.30°).

This solid state structure also exists in solution. The ^{31}P-NMR spectra of both **15** and **16** show an AA′XX′M signal structure, which can be attributed to the pentaphosphine environment surrounding the molybdenum center.

For the complex $[Mo(N_2)(tdppme)(dppm)]$ (**15**), three signals at 43.92, 33.32, and 10.58 ppm are observed (Fig. 10, top).

The multiplet at 43.92 ppm corresponds to the equatorially bound P-donor atoms of the tripod ligand while the signal for the *trans*-phosphine donor can be found at 33.32 ppm. The multiplet at 10.58 ppm is attributed to the P-donor atoms of the dppm ligand. After extraction of the coupling constants, a corresponding ^{31}P-NMR spectrum has been simulated (Fig. 10, bottom). The same signal structure is observed for the complex $[Mo(N_2)(tdppme)(dmpm)]$ (**16**), however, with slightly different chemical shifts.

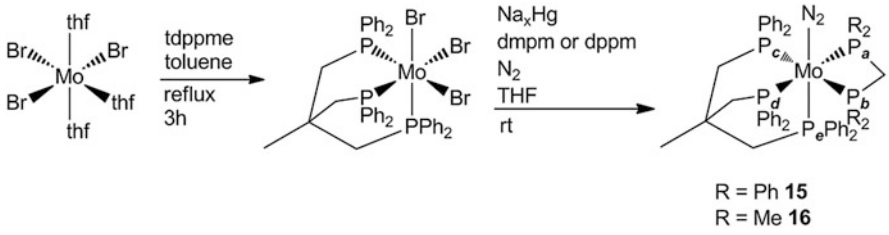

Scheme 9 Synthesis of $[Mo(N_2)(tdppme)(diphos)]$ (**15**, **16**) via reduction of the reactive precursor $[MoBr_3(tdppme)]$ (diphos = dmpm, dppm)

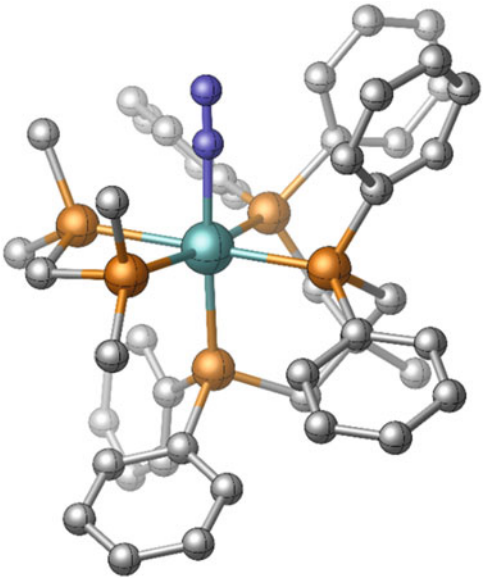

Fig. 9 Single crystal structure of [Mo(N_2)(tdppme)(dmpm)] (**16**). Hydrogen atoms are omitted for clarity [67]

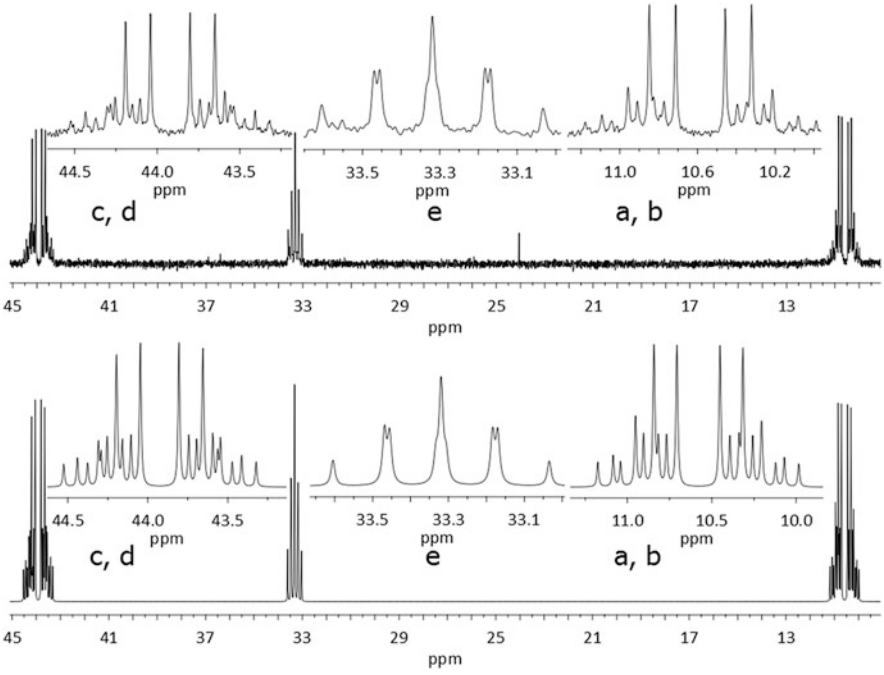

Fig. 10 Comparison of the measured (*top*) and the simulated (*bottom*) ^{31}P-NMR spectrum of [Mo(N_2)(tdppme)(dppm)] (**15**). Simulation of a ^{31}P-NMR spectrum has been carried out after extraction of the coupling constants [67]

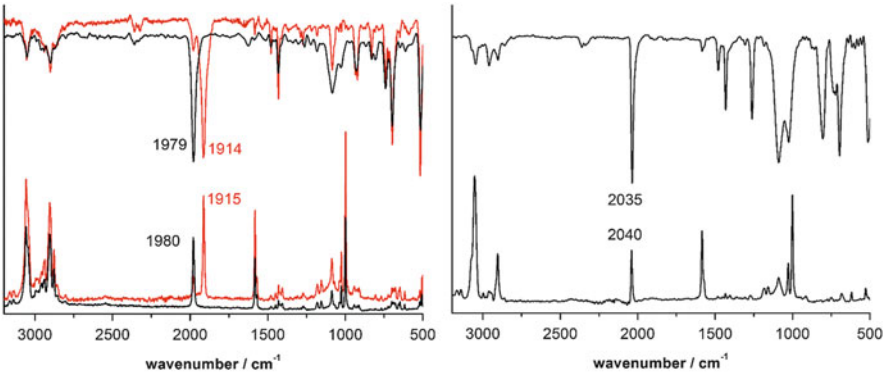

Fig. 11 IR (*top*) and Raman (*bottom*) spectra of [Mo(N_2)(tdppme)(dmpm)] (**16**, *left*, *black*) and [Mo(N_2)(tdppme)(dppm)] (**15**, *right*). *Left*: [Mo($^{15}N_2$)(tdppme)(dmpm)] (^{15}N-**16**) (*red*) [67]

After confirming the constitution of the Mo–N_2 complexes **15** and **16**, the next step was to obtain information regarding the degree of activation of the N_2 ligand. Compared to the free dinitrogen molecule ($\tilde{\nu}_{NN}$ = 2,331 cm^{-1}), moderately activated N_2 complexes exhibit stretching frequencies lower than 2,000 cm^{-1} [86]. While the complex [Mo(N_2)(tdppme)(dmpm)] (**16**) shows an NN stretching frequency at 1,979 cm^{-1} and thus is considered to be activated moderately, the complex [Mo(N_2)(tdppme)(dppm)] (**15**) exhibits a stretching frequency of the coordinated N_2 ligand at 2,035 cm^{-1} and thus is out of the range of moderately activated N_2 complexes (Fig. 11).

Clearly, the coligand has a significant influence on the degree of activation. In order to activate the N_2 ligand, electron density has to be transferred from d orbitals of the metal center to the antibonding orbitals of the dinitrogen ligand which ultimately leads to a weakening of the NN bond. By employing an alkyl phosphine coligand like dmpm, more electron density is donated to the metal center than in case of the dppm coligand. Due to the electron withdrawing character of phenyl groups present in the latter ligand, less electron density is located at the metal center, leading to a shift of $\tilde{\nu}_{NN}$ to higher frequency by 55 cm^{-1}.

The next step was the investigation of the reactivity of the N_2 complexes **15** and **16** towards strong acids. As mentioned above, [Mo(N_2)(tdppme)(dppm)] (**15**), which is less activated than [Mo(N_2)(tdppme)(dmpm)] (**16**), does not exhibit any reactivity towards acids. However, the N_2 ligand of [Mo(N_2)(tdppme)(dmpm)] (**16**) could be protonated using 2 equiv. of trifluoromethanesulfonic acid, leading to the

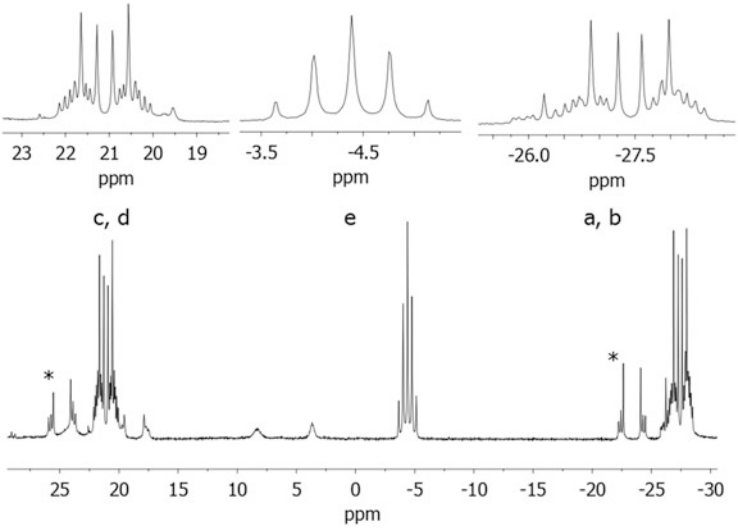

Fig. 12 ^{31}P-NMR spectrum of [Mo(NNH$_2$)(tdppme)(dmpm)](OTf)$_2$ (NNH$_2$-**16**). Signals marked by asterisks at 24.82 and −23.35 ppm (AA′XX′) are probably a consequence of a decomposition product during the NMR measurement [67]

diamagnetic complex [Mo(NNH$_2$)(tdppme)(dmpm)](OTf)$_2$ (NNH$_2$-**16**). The conversion occurred under full retention of the pentaphosphine environment as evidenced by the ^{31}P-NMR spectrum which still exhibits an AA'XX'M signal structure (Fig. 12). In comparison to the parent complex [Mo(N$_2$)(tdppme)(dmpm)] (**16**), all resonances shift to higher field by 10–44 ppm.

Derivatization of N$_2$ in the isotopomer [Mo(^{15}N$_2$)(tdppme)(dmpm)] (^{15}N-**16**) has been carried out as well using 2 equiv. of HOTf. Coupling of the protons of the ^{15}N^{15}NH$_2$ species to the terminal N$_\beta$ atom was detected via ^{1}H-^{15}N HMQC-NMR. With the help of vibrational spectroscopy, more information was obtained regarding the NNH$_2$ species (Fig. 13). Signals at 3,301 and 3,238 cm^{-1} of the complex [Mo(NNH$_2$)(tdppme)(dmpm)](OTf)$_2$ (NNH$_2$-**16**) can be assigned to the antisymmetric and symmetric NH$_2$ stretches. A shift to lower wavenumbers of the NH$_2$ stretch has been detected as well for the ^{15}N$_2$ marked isotopomer [Mo(^{15}N^{15}NH$_2$)(tdppme)(dmpm)](OTf)$_2$ (^{15}N^{15}NH$_2$-**16**; 3,289 cm^{-1} and 3,230 cm^{-1} respectively; Fig. 13). Moreover, the NN stretch of the NNH$_2$ complex can be identified at 1,410 cm^{-1} (Fig. 13).

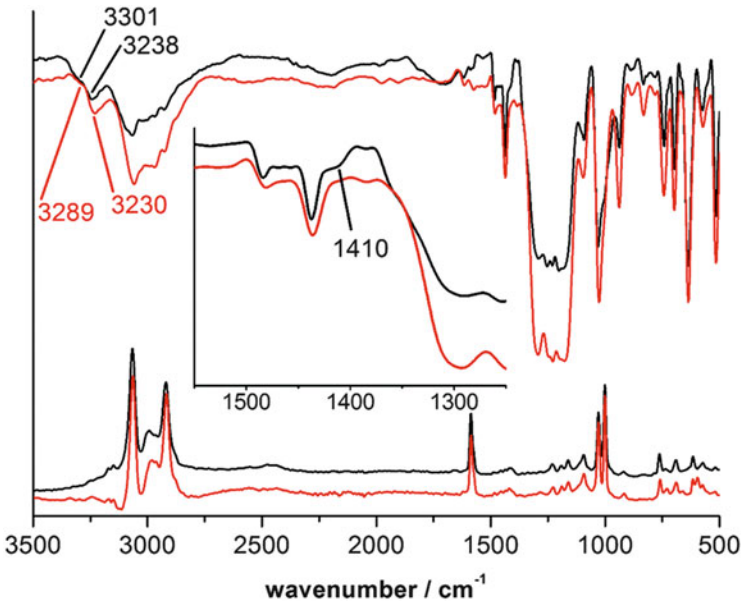

Fig. 13 IR (*top*) and Raman (*bottom*) spectra of [Mo(NNH_2)(tdppme)(dmpm)] (NNH_2-**16**) (*black*) and [Mo($^{15}N^{15}NH_2$)(tdppme)(dmpm)] ($^{15}N^{15}NH_2$-**16**) (*red*). Inset: enlargement of the range of the NN stretching vibration of (NNH_2-**16**) [67]

5 Mo(0)–Dinitrogen Complexes Supported by Hybrid Tripodal Ligands with Mixed Dialkylphosphine/ Diarylphosphine Donor Groups

As shown in the previous section, changing the coligand in tripod-supported molybdenum–dinitrogen complexes from dppm to dmpm leads to a higher activation of N_2 [67]. As a next stage in our investigations of these systems, we also wanted to implement this increase of activation by replacing aryl- by alkylphosphine groups in the tripod ligand. In the framework of this project, we prepared a set of different tripod ligands in which the diphenylphosphine donor groups of tdppme are substituted in a stepwise fashion by diisopropylphosphine groups [68].

By exchanging one diphenylphosphine group of the tdppme ligand by a diisopropylphosphine moiety, the ligand trpd-1 was obtained. The corresponding ligands trpd-2 and trpd-3 possess two and three diisopropylphosphine groups, respectively. Due to preparative reasons, trpd-2 and trpd-3 contain an isobutyl backbone [87]. To investigate the effect of the backbone on the coordination behavior of these ligands, a fourth ligand has been synthesized which contains three diphenylphosphine groups on an isobutyl backbone (Scheme 10) [88]. All four ligands were utilized in combination with the coligands dppm and dmpm to synthesize molybdenum–dinitrogen complexes [69].

Scheme 10 Schematic representation of the substitution pattern of the tripod ligand. Note that the ligands trpd-2, trpd-3, and tdppmm are based on an isobutyl backbone

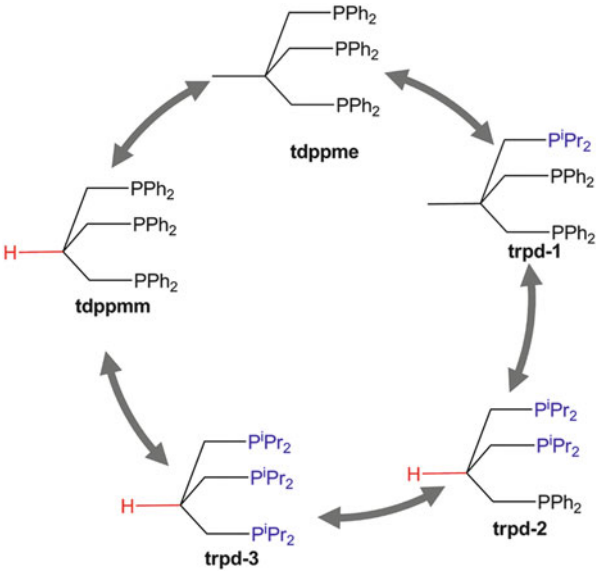

Scheme 11 Representation of the sodium amalgam reduction of the reactive precursor [MoI_3(trpd-1)] in the presence of dmpm or dppm, respectively

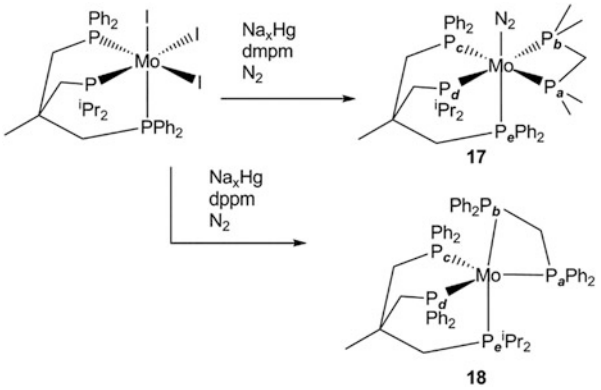

In order to obtain the desired N_2 complexes, the typical procedure has been applied (vide supra). First, the tripod ligands are coordinated to a reactive Mo(III) precursor, secondly a reduction of the molybdenum(III) complexes through sodium amalgam in an N_2 atmosphere with addition of a coligand affords the corresponding Mo–N_2 complexes (Scheme 11). For our set of tripod ligands, we used [$MoI_3(thf)_3$] [55, 89] as a precursor, because it enabled preparation of the Mo(III) tripod complexes in good yields and purities.

Subsequent reduction of the aforementioned complexes by sodium amalgam and addition of the coligand (dppm or dmpm) yielded in cases of trpd-2, trpd-3 and tdppmm complexes with a κ^2-coordination. One explanation for this observation is the high steric demand of the diisopropylphosphine groups incorporated in the

ligands trpd-2 and trpd-3. Another problem is the isobutyl backbone. While the apical methyl group in the neopentyl backbone supports the facial coordination of the tripod ligand, the isobutyl backbone does not possess this methyl group. Because the pivotal *trans*-position to N_2 is not saturated by the ligand, the κ^2-complexes are not suitable for further investigations.

Interestingly, sodium amalgam reduction of [MoI_3(trpd-1)] precursor and dppm as coligand resulted in a molybdenum complex without coordinated dinitrogen. Although the ^{31}P-NMR spectrum showed five sets of signals, which are indicative of five different phosphorus species coordinated to the metal center, no signals or traces of dinitrogen could be found by elemental analysis or vibrational spectroscopy. Thus the complex [Mo(trpd-1)(dppm)] (**18**) has been obtained which possesses a rare fivefold coordination, certainly due to the high steric demand of the P^iPr_2 [90] group and the bigger coligand dppm.

On the other hand, a six-coordinate Mo(0)–N_2 complex has been successfully synthesized with trpd-1 and dmpm as coligand. Single crystal X-ray structure analysis of this complex (**17**) shows that the diisopropylphosphine group is located in the equatorial plane, i.e., *cis* to the axial N_2 ligand. As expected, the structure determination proved the existence of five coordinated phosphine donor groups besides the N_2 ligand. Compared to the symmetric tdppme complex **16**, the trpd-1 complex **17** possesses a distorted octahedral structure (Fig. 14).

^{31}P-NMR spectroscopy has been applied to gain further information concerning the structure of the complex (Fig. 15). This spectrum shows different sets of dddd-signals which can be found at 47.3, 41.1, 40.3, and −24.5 ppm. The signals at −24.5 ppm can be ascribed to the P atoms of the dmpm coligand and are in the range of our previous result for [Mo(N_2)(tdppme)(dmpm)] (**16**) [67]. The signal at 40.3 ppm corresponds to the diphenylphosphine group *trans* to the N_2 ligand of the

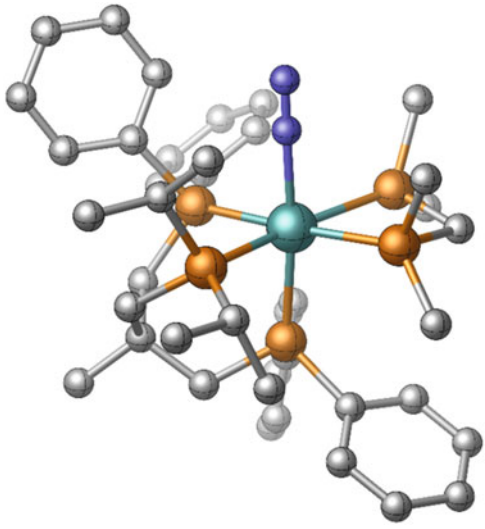

Fig. 14 Single crystal structure of [Mo(N_2)(trpd-1)(dmpm)] (**17**). Hydrogen atoms are omitted for clarity [69]

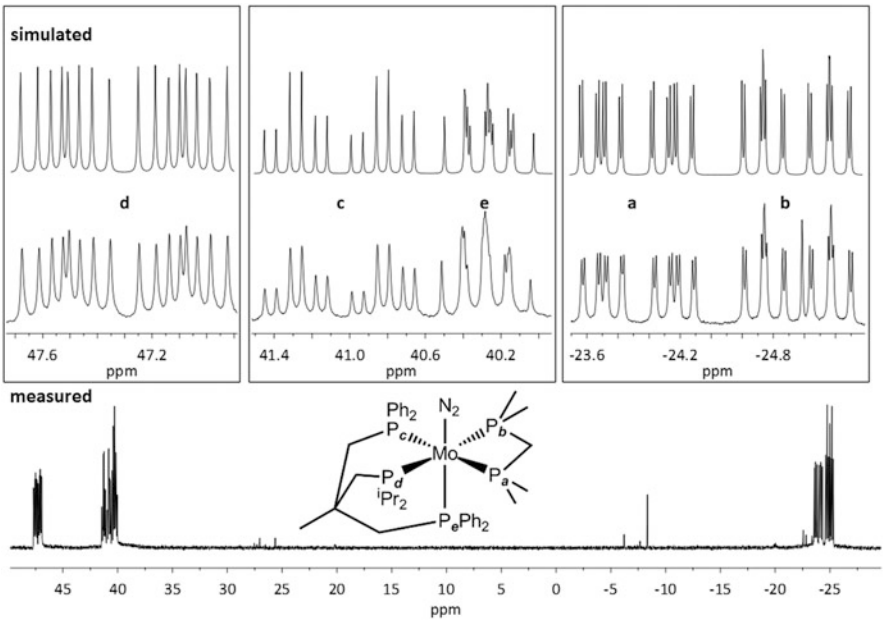

Fig. 15 ^{31}P-NMR of [Mo(N_2)(trpd-1)(dmpm)] (**17**) with the detailed zoom for the simulation (*top*) and the measurement (*bottom*) [69]

complex. The second diphenylphosphine group can be found at 41.1 ppm, while the signal of the diisopropylphosphine group is located at 47.3 ppm (Fig. 15).

IR and Raman spectra of the dinitrogen complex **17** show an NN stretch at 1,965 cm^{-1} which is in the range of moderately activated dinitrogen complexes. Moreover, the additional alkylphosphine group of the aforementioned complex increased the activation of the N_2 ligand compared to the parent system [Mo(N_2)(tdppme)(dmpm)] (**16**) ($\tilde{\nu}_{NN}$ = 1,979 cm^{-1}) [67].

The reactivity of this complex towards acids has been investigated as well. Although several experiments with HOTf, H_2SO_4, or HCl have been performed, the desired NNH_2 complex could not be obtained. However, application of $HBAr^F$ [91] led to generation and detection of the NNH_2 species under retention of the pentaphosphine coordination, as evidenced by subsequent ^{31}P-NMR measurement.

Obviously, $HBAr^F$ is a suitable acid for this experiment because of the non-coordinating anion (Scheme 12). The signals of the complex [Mo(NNH_2)(trpd-1)(dmpm)](BAr^F)$_2$ (NNH_2-**17**) are shifted to high field as evidenced before for the complex [Mo(NNH_2)(tdppme)(dmpm)](OTf)$_2$ (NNH_2-**16**) (Fig. 16).

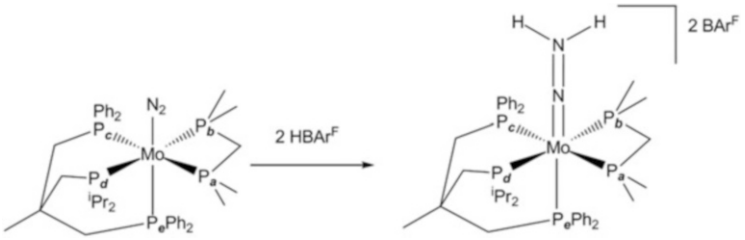

Scheme 12 Derivatization of the ligand N_2 by using 2 equiv. of the acid $HBAr^F$

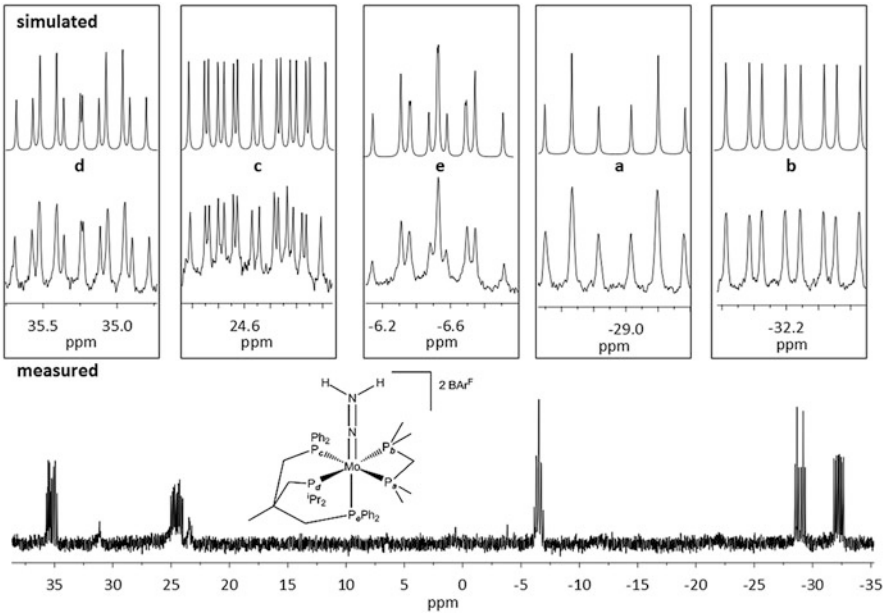

Fig. 16 ^{31}P-NMR of [Mo(NNH_2)(trpd-1)(dmpm)] (NNH_2-**17**) with detailed zoom of the simulated (*top*) and measured (*bottom*) spectra [69]

6 Mo(0)–Dinitrogen Complexes Supported by Tetradentate NP_3 Ligands

A further approach towards occupying the *trans*-position of a dinitrogen ligand in molybdenum–dinitrogen complexes is based on tetradentate NP_3 ligands. Towards this goal, our group synthesized the new tetradentate ligands prNP_3 (NP_3 = $N(CH_2CH_2CH_2PPh_2)_3$) and prPNetP_2 (prPNetP_2 = $(Ph_2PCH_2CH_2CH_2)N(CH_2CH_2PPh_2)_2$) (Scheme 13). The ligand prPNetP_2 is an asymmetric ligand which contains mixed ethylene/propylene bridges. The coordination of these ligands to molybdenum(0) centers and their impact to the activation of the N_2 ligand have been studied [48].

Scheme 13 The tetradentate $prNP_3$ (*left*) and $prPNetP_2$ ligand (*right*)

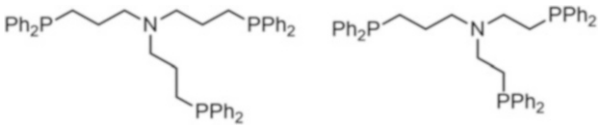

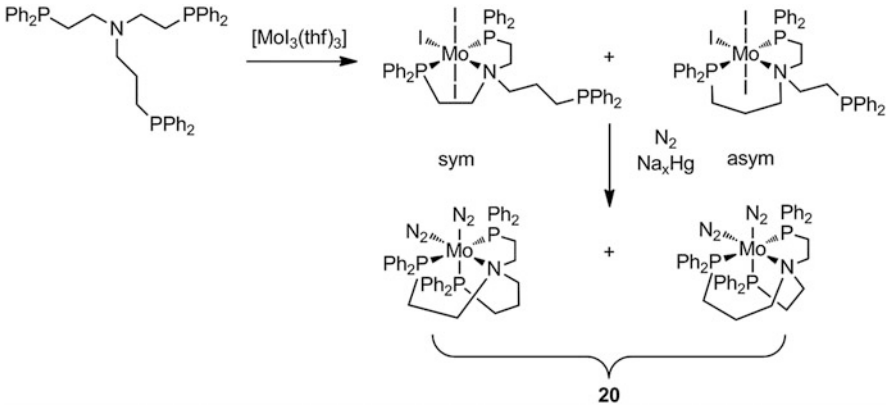

Scheme 14 Synthesis of the complexes $[MoI_3(prPNetP_2)]$ and $[Mo(N_2)_2(prPNetP_2)]$ (**20**)

To obtain Mo(0)–dinitrogen complexes, we first synthesized the Mo(III) complexes $[MoCl_3(prNP_3)]$ and $[MoI_3(prPNetP_2)]$ by reaction of $prNP_3$ and $prPNetP_2$ with $[MoCl_3(thf)_3]$ and $[MoI_3(thf)_3]$. Reduction of the respective Mo(III) complexes with sodium amalgam in a dinitrogen atmosphere led to the *cis*-bis(dinitrogen) Mo(0) complexes $[Mo(N_2)_2(prNP_3)]$ (**19**) and $[Mo(N_2)_2(prPNetP_2)]$ (**20**). The synthesis of the latter is shown in Scheme 14 [48].

Reaction of the asymmetric $prPNetP_2$ ligand with the Mo(III) precursor $[MoI_3(thf)_3]$ leads to formation of two isomers: (1) *sym* (coordination of $prPNetP_2$ by two ethylene bridged phosphines) and (2) *asym* (coordination of $prPNetP_2$ by one ethylene and one propylene bridged phosphines; Scheme 14). With the help of DFT calculations, we found out that the *sym*-isomer is energetically disfavored by 7.4 kcal mol^{-1} [48]. Reduction with Na_xHg generates the corresponding dinitrogen complexes, which also exist in different isomeric forms (vide infra). Importantly, we observed a κ^4-coordination of the new ligands $prPNetP_2$ and $prNP_3$ for all bis-(dinitrogen) Mo(0) complexes in solution. However, the thermal stability of the new complexes is limited [48].

The new Mo(0)–dinitrogen complexes $[Mo(N_2)_2(prNP_3)]$ (**19**) and $[Mo(N_2)_2(prPNetP_2)]$ (**20**) were characterized by vibrational and NMR spectroscopy [48]. The IR spectrum of $[Mo(N_2)_2(prNP_3)]$ (**19**) shows a symmetric (1,950 cm^{-1}) and an antisymmetric (1,904 cm^{-1}) combination of NN vibrations, reflecting a moderate activation of N_2. The relative intensities of the two vibrations indicate that the *cis*-bis(dinitrogen) complex **19** was obtained [48]. It was expected that in the ^{31}P-NMR spectrum of $[Mo(N_2)_2(prNP_3)]$ (**19**) an A_2M spin system appears, similar to the literature-known complex *cis*-$[Mo(N_2)_2(NP_3)]$ (**21**) of Fernández-Trujillo et al.

($NP_3 = N(CH_2CH_2PPh_2)_3$ [48]. However, in place of an A_2M spin system an AMX system was observed (Fig. 17) [48].

The observation of the AMX spectrum can be explained by DFT. In Fig. 18, the geometry optimized structures of *cis*-[$Mo(N_2)_2(NP_3)$] (**21**) and [$Mo(N_2)_2(prNP_3)$] (**19**) are shown. In the structure of *cis*-[$Mo(N_2)_2(NP_3)$] (**21**) (Fig. 18, left), the phosphines *trans* to each other are symmetric with respect to a plane containing both dinitrogen ligands and thus are magnetically equivalent. In contrast, the optimized structure of [$Mo(N_2)_2(prNP_3)$] (**19**) (Fig. 18, right) shows a rotation of the $prNP_3$ ligand around the N–Mo–N_2 axis. Therefore the phosphines *trans* to each other are not equivalent anymore. Breaking the mirror symmetry of the parent complex **21** is the reason for the splitting of the signals in the ^{31}P-NMR spectrum (Fig. 19) [48].

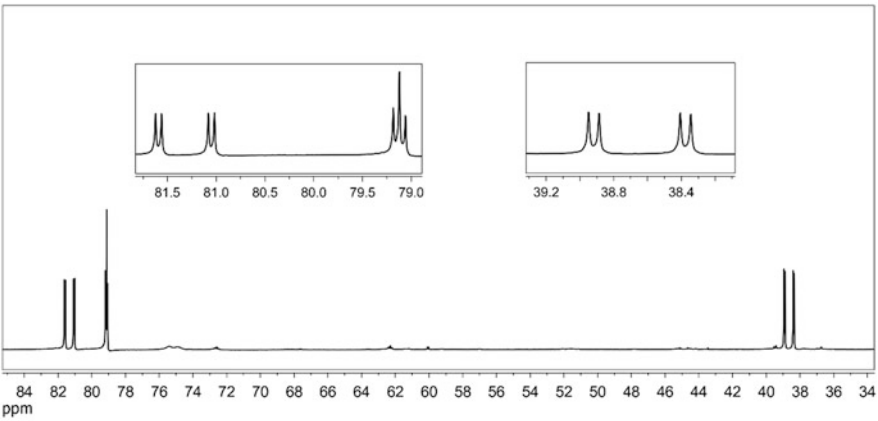

Fig. 17 ^{31}P-NMR spectrum of [$Mo(N_2)_2(prNP_3)$] (**19**) [46]

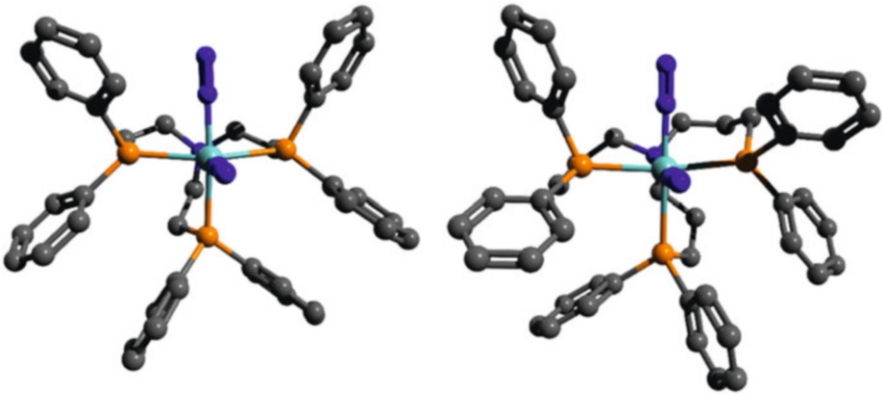

Fig. 18 Geometry optimized structures of [$Mo(N_2)_2(NP_3)$] (**21**, *left*) and [$Mo(N_2)_2(prNP_3)$] (**19**, *right*) [46]

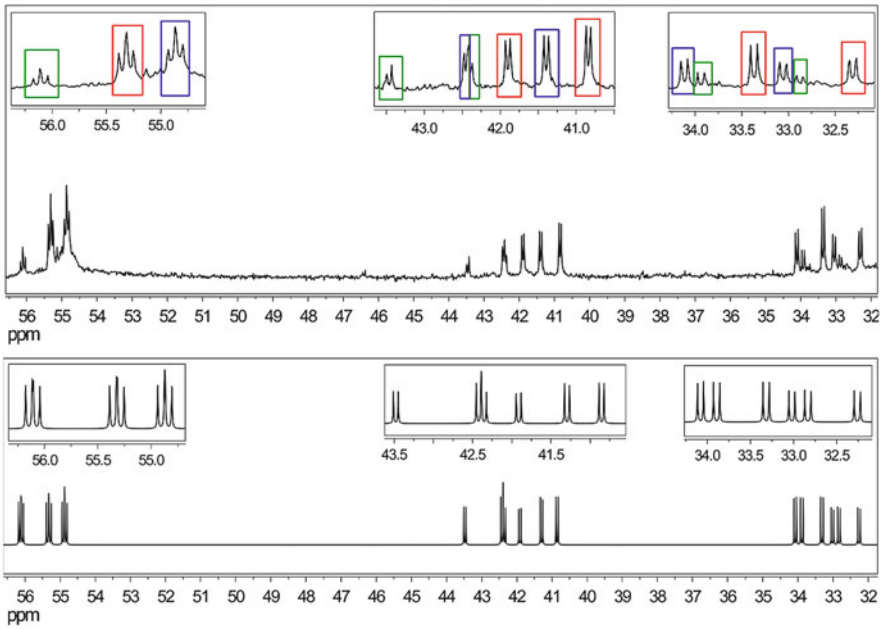

Fig. 19 ^{31}P-NMR spectrum of [Mo(N_2)$_2$(prPNetP$_2$)] (**20**) (*top*: measured; *bottom*: simulated). Three types of frames (*green*, *red*, and *blue*) indicate the AMX subspectra of three species [48]

The IR spectrum of [Mo(N_2)$_2$(prPNetP$_2$)] (**20**) exhibits a symmetric (1,991 cm^{-1}) and an antisymmetric (1,925 cm^{-1}) stretching vibration of the N_2 ligands. Again, the relative intensities indicate that the *cis*-bis(dinitrogen) complex is formed [48]. In the ^{31}P-NMR spectrum of **20** (Fig. 19), three AMX patterns are observed. Due to the appearance of AMX systems, it can be inferred that the two phosphines *trans* to each other are magnetically inequivalent (vide supra) [48]. The observation of three AMX patterns leads to the conclusion that three different isomers of the complex **20** have been formed during the reaction.

With the help of DFT calculations, more information about the structure of possible isomers was obtained. The geometry optimized structures are shown in Figs. 20 and 21. All these isomers differ with respect to the configuration of the C_3 bridge relative to the *cis*-C_2 bridge. The calculated relative energies (in kcal mol^{-1}) for the *asym*-isomers are 0 for **20e**, +0.28 for **20b**, +2.22 for **20c**, +3.94 for **20d**, and for the *sym*-isomer (**20a**) +2.53 [48].

Probably, all of the signals in the ^{31}P-NMR spectrum belong to the *asym* form of the [Mo(N_2)$_2$(prPNetP$_2$)] complex (**20**). In the *asym* form, the ethylene and propylene bridges are located within the PNP plane and a mirror plane is lacking. Comparing the *trans* coupling constant of the phosphorus nuclei in [Mo(N_2)$_2$(prPNetP$_2$)] (**20**) with the equivalent phosphorus species in [Mo(N_2)$_2$(prNP$_3$)] (**19**), it can be noted that the coupling constants are significantly different. On the other hand, the respective coupling constants of the three isomers are nearly equal. If one of the isomers was

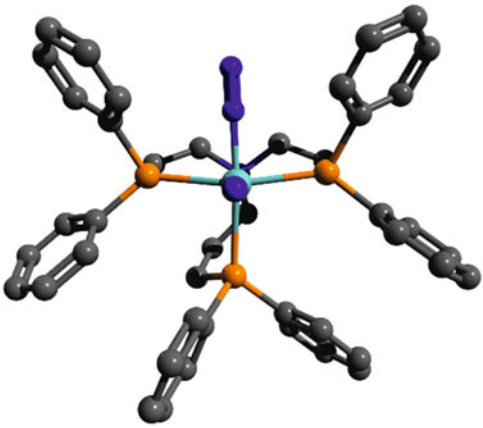

Fig. 20 Optimized structure of the isomer of *sym*-[$Mo(N_2)_2$(prPNetP_2)] (**20a**) [48]

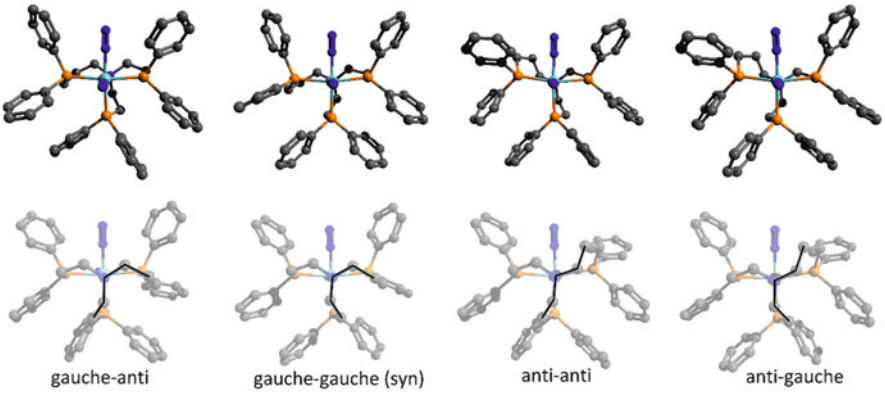

Fig. 21 Optimized structures of the four possible isomers of *asym*-[$Mo(N_2)_2$(prPNetP_2)] (*asym*-**20**) (*left* to *right*: **20b**, **20c, 20d**, and **20e**). *Top*: front view; *bottom*: rear view with indication of the conformation [48]

the *sym*-isomer, we would observe one different *trans* coupling constant. Therefore we assume that the three species observed in the ^{31}P-NMR spectrum are *asym*-isomers. Maybe the product distribution of the Mo(0) complexes is also influenced by the Mo(III) precursor, where the *sym*-isomer is disfavored (vide supra) [48].

According to the DFT calculations, the formation of four *asym*-isomers is in principle possible (**20b–e**, Fig. 21), but only three sets of AMX signals are apparent in the ^{31}P-NMR spectrum (Fig. 19). Compound **20d** is the energetically least favorable product; consequently, we assume that this complex is not formed during the reaction [48].

7 Mo(0)–Dinitrogen Complex Supported by a Pentadentate Tetrapodal Phosphine (pentaPod^{P}) Ligand

In the preceding sections, several possibilities to occupy the *trans*-position of coordinated N_2 in Chatt type systems have been explored. Our first attempt towards this goal was based on complexes with a combination of a trident and a diphos ligand as present in, e.g., [Mo(N_2)(dpepp)(dppm)] [41]. Then, in order to ensure a higher stability of the phosphine environment, the use of tripod ligands was explored. The neopentyl backbone enforces a facial coordination of these ligands [67, 69, 70]. However, also in these systems the phosphine group in the axial position to the N_2 ligand was found to be prone to dissociation, leading to coordination of external ligands such as the conjugated base of the acid employed for protonation or a solvent molecule. The ultimate solution to this problem is the synthesis of a pentadentate tetrapodal phosphine (pentaPod^{P}) ligand [92]. This type of ligand derives from the fusion of a tripod and a trident ligand (Fig. 22).

The synthesis of the pentaPod^{P} ligand is shown in Scheme 15. The trident part of the ligand is composed of bis(3-(diphenylphosphino)propyl)phosphine (prPPHP) which has already been presented in Sect. 2. The synthesis of the tripod part starts

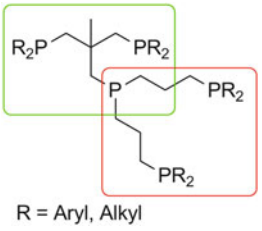

Fig. 22 The pentaPod^{P} ligand consists of a tripodal part (*green*) and a tridentate part (*red*)

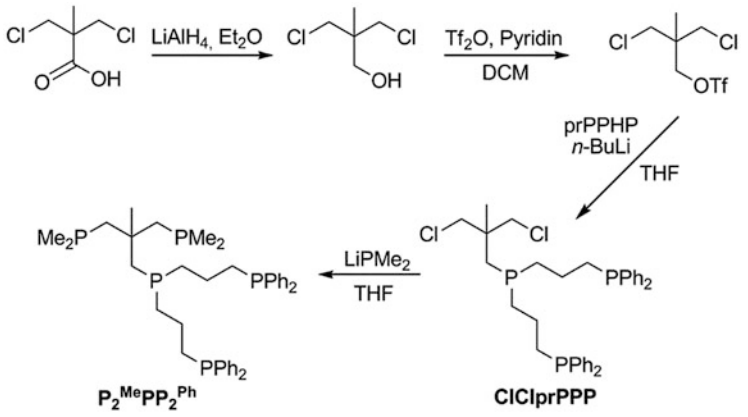

Scheme 15 Synthesis of the pentapod^{P} ligand $P_2{}^{Me}PP_2{}^{Ph}$

from 3,3-dichloropivalic acid. After reduction of the acid function and the conversion of the resulting alcohol residue to the triflate [93], prPPLiP was reacted with the triflate function of the tripod part to yield the proligand ClClprPPP. The last step of the reaction required 2 eq. of $LiPMe_2$ which reacted with ClClprPPP to ultimately produce the pentaPod^P ligand $P_2{}^{Me}PP_2{}^{Ph}$ [92].

Coordination of the pentadentate phosphine ligand ($P_2{}^{Me}PP_2{}^{Ph}$) was achieved by addition of an equimolar amount of $[MoCl_3(thf)_3]$ [50, 92, 94]. Due to the incorporation of different phosphine donor groups in the trident and the tripod part of the ligand (alkyl vs. aryl phosphines), the pentaPod^P ligand possesses a unique coordination behavior. While the tripod part inevitably leads to a facially coordinated product, coordination of the trident part is more likely to result in a complex with a meridional isomer [67, 95]. It is expected that the tripod part of $P_2{}^{Me}PP_2{}^{Ph}$ coordinates selectively to $[MoCl_3(thf)_3]$, yielding *fac*(trpd)-$[MoCl_3(P_2{}^{Me}PP_2{}^{Ph})]$ (trpd = tripod) (Scheme 16). This is a consequence of the stronger σ-donor character and the smaller steric demand of the dimethylphosphines in comparison to the diphenylphosphine donor groups. Subsequent sodium amalgam reduction of *fac*(trpd)-$[MoCl_3(P_2{}^{Me}PP_2{}^{Ph})]$ leads to a mononuclear dinitrogen complex with coordination of the remaining diphenylphosphine donor groups of the trident part of the ligand [92].

This way, the desired pentaphosphine environment, which is necessary to minimize the shortcomings of Chatt type systems, has been achieved by the employment of just one ligand. The structure of **22** was proven by ^{31}P-NMR spectroscopy and single crystal structure determination. As explained earlier, an AA′XX′M signal structure in the ^{31}P-NMR spectrum is expected for a complex with five coordinated phosphine donors (Fig. 23). After extraction of the necessary coupling constants, a simulation has been performed [96].

A further proof for the structure of **22** was obtained by single crystal X-ray structure determination (Fig. 24). The data clearly show the pentaPod^P ligand occupying five coordination sites of the molybdenum center and the dinitrogen ligand binding to the remaining coordination site. The activation of N_2 in the complex $[Mo(N_2)(P_2{}^{Me}PP_2{}^{Ph})]$ (**22**) leads to an elongation of the $N_\alpha N_\beta$ distance (1.099(5) Å) compared to elemental N_2 (1.0975 Å).

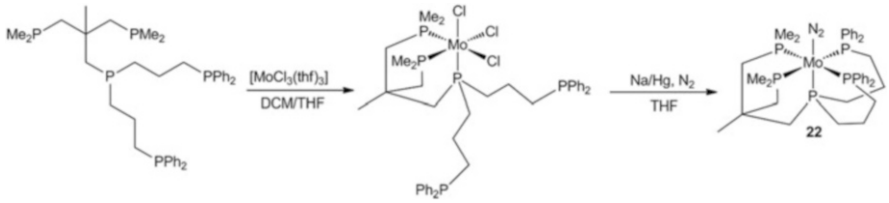

Scheme 16 Coordination of the pentaPod^P ligand $P_2{}^{Me}PP_2{}^{Ph}$ on $[MoCl_3(thf)_3]$ and subsequent sodium amalgam reduction under the atmosphere of N_2 to generate the molybdenum–dinitrogen complex $[Mo(N_2)(P_2{}^{Me}PP_2{}^{Ph})]$ (**22**)

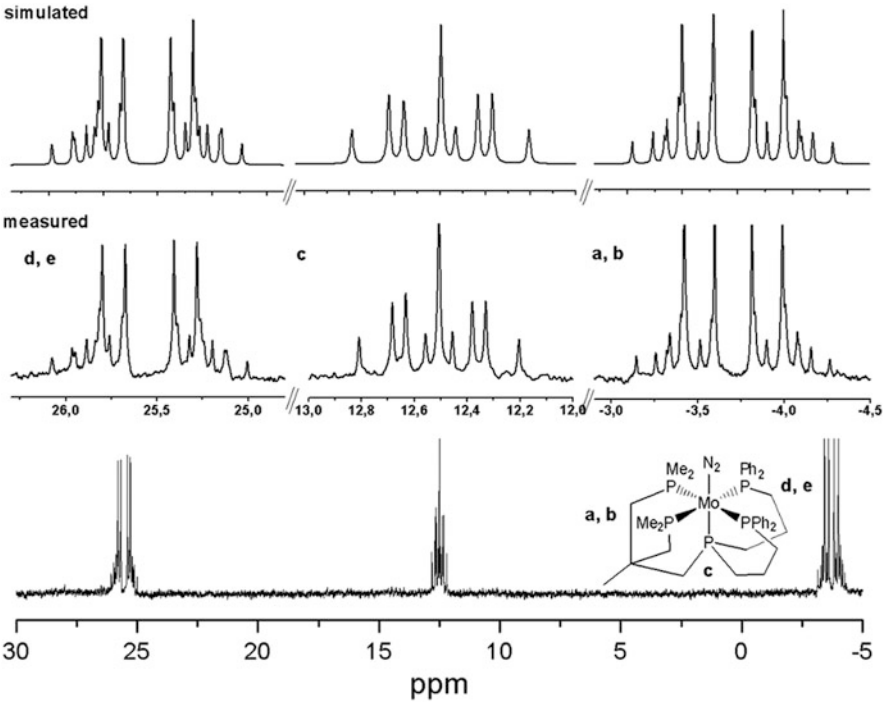

Fig. 23 ^{31}P-NMR spectrum of [Mo(N_2)($P_2^{Me}PP_2^{Ph}$)] (**22**) (*bottom*) with magnifications of the simulation (*top*) and the measurement (*middle*) [92]

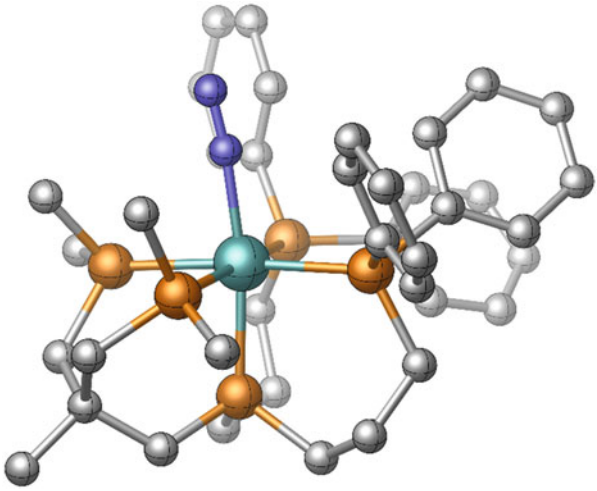

Fig. 24 Crystal structure of [Mo(N_2)($P_2^{Me}PP_2^{Ph}$)] (**22**). Hydrogen atoms are omitted for clarity [92]

While the bond lengths between the equatorially bound phosphine donor atoms and the molybdenum atom (Mo-P_{eq}) exhibit an average value of 2.4481 Å, the phosphine donor atom located *trans* to the dinitrogen ligand shows quite a short bond length (2.3868(5) Å) to the metal center. This proves the successful strapping of the central phosphine donor in the pentaPod^{P} design. The strong Mo–P_{ax} bond hinders dissociation at this position, solving one of the problems of the original Chatt systems [92].

IR and Raman spectra were measured to examine the degree of activation of the coordinated dinitrogen ligand (Fig. 25). The spectra show an NN stretching vibration at 1,929 cm^{-1}. To the best of our knowledge, this is the lowest value of an NN stretch for a mononuclear molybdenum–dinitrogen complex with phosphine ligands. For comparison and further characterization, the $^{15}N_2$-complex of [Mo(N_2)($P_2^{Me}PP_2^{Ph}$)] (**22**) has been synthesized as well. The NN stretching frequency of [Mo($^{15}N_2$)($P_2^{Me}PP_2^{Ph}$)] (^{15}N-**22**) is observed at 1,868 cm^{-1}. Theoretically ($\Delta_{theo} = 65\ cm^{-1}$) and experimentally determined ($\Delta_{exp} = 61\ cm^{-1}$) isotope shifts are in good agreement [92].

The reactivity of the complex [Mo(N_2)($P_2^{Me}PP_2^{Ph}$)] (**22**) towards acids was investigated as well. For the protonation reactions, two different acids have been employed, HOTf and HBAr^{F} [92]. Protonation with trifluoromethanesulfonic acid in THF was unsuccessful because ligand-exchange reactions with solvent molecules took place. Analysis of the protonation products was performed using NMR and IR

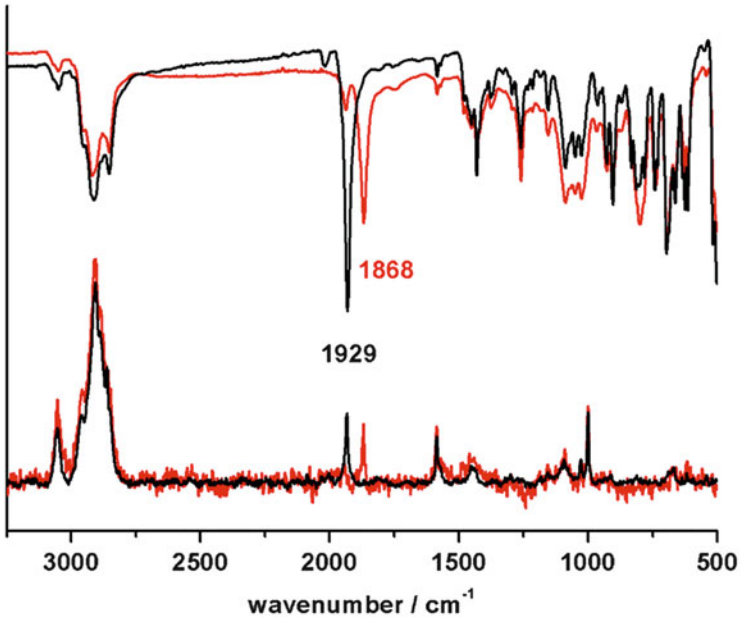

Fig. 25 Comparison of IR and Raman spectra of [Mo(N_2)($P_2^{Me}PP_2^{Ph}$)] (**22**) (*black*) and [Mo($^{15}N_2$)($P_2^{Me}PP_2^{Ph}$)] (^{15}N-**22**) (*red*) [92]

spectroscopy [12, 69]. It was possible to characterize the [Mo(NNH$_2$)(P$_2$^{Me}PP$_2$^{Ph})] (NNH$_2$-**22**) species at a temperature of 250 K, whereas it became unstable at 270 K. The ^{31}P-NMR spectrum of NNH$_2$-**22** shows a shift of the signals to high field compared to **22**; in particular, a shift for *trans*-phosphine by 45.9 ppm has been observed (Fig. 26). Moreover, a signal at −234 ppm could be obtained from ^{15}N-INEPT-NMR spectroscopy, reflecting a doubly protonated N$_\beta$ atom, which indicates a successful protonation experiment [97, 98].

In situ IR investigations revealed that upon protonation the NN stretch at 1,929 cm^{-1} disappears and two new NH stretching vibrations emerge at 3,198 cm^{-1} and 3,179 cm^{-1}, respectively (Fig. 27) [67]. Again, these findings indicate formation of the NNH$_2$ complex.

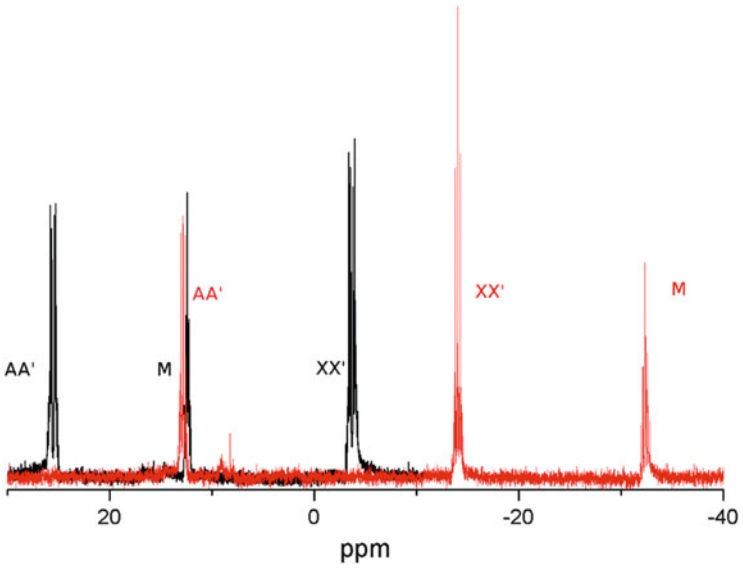

Fig. 26 Comparison of ^{31}P-NMR spectra of [Mo(N$_2$)(P$_2$^{Me}PP$_2$^{Ph})] (**22**) (*black*) and [Mo(NNH$_2$)(P$_2$^{Me}PP$_2$^{Ph})](NNH$_2$-**22**) (*red*). All signals undergo a downfield shift which is most significant for the M signal [92]

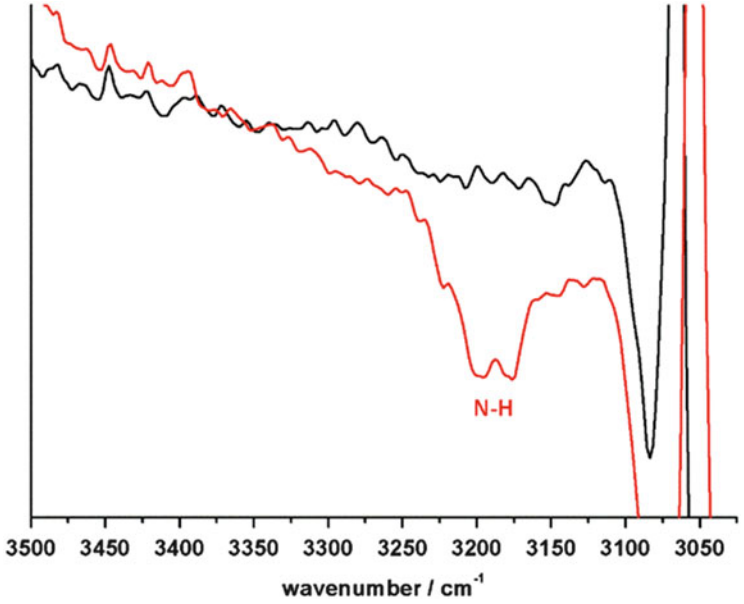

Fig. 27 Comparison of the NH-vibration regions of Mo-N_2- (**22**, *black*) and Mo-NNH_2- (NNH_2-**22**, *red*) complexes. The protonation was carried out with $HBAr^F$ [92]

8 Summary and Conclusion

In the present review, our synthetic efforts towards the development of an efficient catalyst for N_2 reduction on the basis of mononuclear Mo(0) phosphine complexes are described. One of the major problems of the Chatt system is the disproportionation reaction at the level of the Mo(I) complex which is caused by the coordination of an anionic ligand in *trans*-position of the N_2 ligand. To prevent this problematic reaction, the *trans*-position must be blocked by the ligand system. Several concepts to achieve this goal have been pursued. Our first approach involved the use of PEP ligands with the donor atom E (N, P) in *trans*-position to N_2. Interestingly, dinitrogen complexes with PNP ligands exhibited a much higher activation of N_2 than their analogues supported by PPP ligands. Then, complexes with PCP ligands were examined, the central carbon donor being contained in an N-heterocyclic carbene. Importantly, the presence of a carbene donor in *trans*-position of N_2 caused a dramatic increase in the activation of this ligand. On the other hand, the corresponding dinitrogen complexes became thermally unstable, which could be remedied by employing phosphite instead of phosphine coligands.

A major focus in our investigations has also been directed towards the synthesis of molybdenum–dinitrogen complexes supported by tripod ligands. We started these investigations with the commercially available ligand tris(diphosphinomethyl)ethane (tdppme), complemented by dppm and dmpm coligands. Later on, we also replaced the diphenylphosphine endgroups of the tdppme ligand by aliphatic phosphine groups

PR_2, starting with R = isopropyl substituents. The resulting Mo(0)–dinitrogen complexes exhibited a greater activation of N_2 than their tdppme-supported counterparts, but the accommodation of more than one diisopropylphosphine group in the tripod ligand proved to be difficult.

The ultimate stage of our studies involved the development of pentaPod^P ligands which derive from the fusion of a PEP and a tripod ligand. Importantly, this ligand contains PMe_2 groups on the tripod and PPh_2 groups on the trident part of the pentaPod backbone. This allows a stepwise coordination of this ligand to Mo centers, leading to the first molybdenum–dinitrogen complex supported by a pentadentate tetrapodal phosphine ligand.

An important aspect in the design of these multidentate phosphine ligands is the proper choice of the chain length in tridentate PEP ligands and the tridentate parts of pentaPod^P ligands, respectively. This problem has both been investigated on the basis of the above-mentioned, tridentate PNP/PPP ligands and on the basis of tetradentate NP_3 ligands. While the replacement of C_2 by C_3 groups has little influence on the activation of N_2 in Mo(0) complexes supported by these types of ligands, the presence of C_3 bridges leads to a higher flexibility of the ligand framework which is reflected by the appearance of conformers and/or line broadening in the ^{31}P-NMR spectra. With regard to the pentaPod^P design, the use of C_3 bridges in the trident part appears to provide a stable, yet flexible coordination environment. The reactivity of the [Mo(N_2)(pentaPod^P)] complex **22** towards acids and reductants now is being studied in detail, as well as the conversion of N_2 to ammonia on the basis of this system.

References

1. MacKay BA, Fryzuk MD (2004) Chem Rev 104:385–401
2. Burgess BK, Lowe DJ (1996) Chem Rev 96:2983–3011
3. Alberty RA, Goldberg RN (2004) Biochemistry 31:10610–10615
4. Burgess BK (1990) Chem Rev 90:1377–1406
5. Kim JS, Rees DC (1992) Nature 360:553–560
6. Lancaster KM, Roemelt M, Ettenhuber P, Hu Y, Ribbe MW, Neese F, Bergmann U, DeBeer S (2011) Science 334:974–977
7. Spatzal T, Aksoyoglu M, Zhang L, Andrade SLA, Schleicher E, Weber S, Rees DC, Einsle O (2011) Science 334:940–940
8. Thorneley RNF, Lowe DJ (1985) In: Spiro TG (ed) Molybdenum enzymes. Wiley, New York
9. Hinrichsen S, Broda H, Gradert C, Söncksen L, Tuczek F (2012) Annu Rep Prog Chem Sect A Inorg Chem 108:17–47
10. Henderson RA, Leigh GJ, Pickett CJ (1983) Adv Inorg Chem 27:197–292
11. Arashiba K, Kinoshita E, Kuriyama S, Eizawa A, Nakajima K, Tanaka H, Yoshizawa K, Nishibayashi Y (2015) J Am Chem Soc 137:5666–5669
12. Del Castillo TJ, Thompson NB, Peters JC (2016) J Am Chem Soc 138:5341–5350
13. Schrock RR (2005) Acc Chem Res 38:955–962
14. Yandulov CV, Schrock RR (2003) Science 301:76–78
15. Arashiba K, Miyake Y, Nishibayashi Y (2011) Nat Chem 3:120–125
16. Kinoshita E, Arashiba K, Kuriyama S, Miyake Y, Shimazaki R, Nakanishi H, Nishibayashi Y (2012) Organometallics 31:8437–8443

17. Kuriyama S, Arashiba K, Nakajima K, Tanaka H, Kamaru N, Yoshizawa K, Nishibayashi Y (2014) J Am Chem Soc 136:9719–9731
18. Nishibayashi Y (2015) C R Chim 18:776–784
19. Anderson JS, Rittle J, Peters JC (2013) Nature 501:84–87
20. Chatt J, Dilworth JR, Richards RL (1978) Chem Rev 78:589–625
21. Chatt J, Pearman AJ, Richards RL (1975) Nature 253:39–40
22. Hidai M, Tominari K, Uchida Y, Misono A (1969) J Chem Soc D Chem Commun:1392
23. Hidai M, Tominari K, Uchida Y (1972) J Am Chem Soc 94:110–114
24. Hidai M, Mizobe Y (1995) Chem Rev 95:1115–1133
25. Broda H, Hinrichsen S, Tuczek F (2013) Coord Chem Rev 257:587–598
26. Dreher A, Stephan G, Tuczek F (2009) Adv Inorg Chem 61:367–405
27. Römer R, Stephan G, Habeck C, Hoberg C, Peters G, Näther C, Tuczek F (2008) Eur J Inorg Chem 21:3258–3263
28. Römer R, Gradert C, Bannwarth A, Peters G, Näther C, Tuczek F (2011) Dalton Trans 40:3229–3236
29. Söncksen L, Römer R, Näther C, Peters G, Tuczek F (2011) Inorg Chim Acta 374:472–479
30. Lehnert N, Tuczek F (1999) Inorg Chem 38:1659–1670
31. Lehnert N, Tuczek F (1999) Inorg Chem 38:1671–1682
32. Horn KH, Lehnert N, Tuczek F (2003) Inorg Chem 42:1076–1086
33. Horn KH, Böres N, Lehnert N, Mersmann K, Näther C, Peters G, Tuczek F (2005) Inorg Chem 44:3016–3030
34. Mersmann K, Horn KH, Böres N, Lehnert N, Studt F, Paulat F, Peters G, Ivanovic-Burmazovic I, van Eldik R, Tuczek F (2005) Inorg Chem 44:3031–3045
35. Mersmann K, Hauser A, Lehnert N, Tuczek F (2006) Inorg Chem 45:5044–5056
36. Dreher A, Mersmann K, Näther C, Ivanovic-Burmazovic I, van Eldik R, Tuczek F (2009) Inorg Chem 48:2078–2093
37. Dreher A, Meyer S, Näther C, Westphal A, Broda H, Sarkar B, Kaim W, Kurz P, Tuczek F (2013) Inorg Chem 52:2335–2352
38. Stephan G, Sivasankar C, Studt F, Tuczek F (2008) Chem A Eur J 14:644–652
39. George TA, Tisdale RC (1988) Inorg Chem 27:2909–2912
40. George TA, Ma L, Shailh SN, Tisdale RC, Zubieta J (1990) Inorg Chem 29:4789–4796
41. Stephan G, Peters G, Lehnert N, Habeck CM, Näther C, Tuczek F (2005) Can J Chem 83:385–402
42. George TA, Jackson MA (1988) Inorg Chem 27:924–926
43. Weiss CJ, Groves AN, Mock MT, Dougherty WG, Kassel WS, Helm ML, DuBois DL, Bullock RM (2012) Dalton Trans 41:4517–4529
44. Ogawa T, Kajita Y, Wasada-Tsutsui Y, Wasada H, Masuda H (2013) Inorg Chem 52:182–195
45. Stephan G, Näther C, Sivasankar C, Tuczek F (2008) Inorg Chim Acta 361:1008–1019
46. Hinrichsen S, Schnoor AC, Grund K, Flöser B, Schlimm A, Näther C, Krahmer J, Tuczek F (2016) Dalton Trans 45:14801–14813
47. Fernández-Trujillo MJ, Basallote MG, Valerga P, Puerta MC (1993) J Chem Soc Dalton Trans:923–926
48. Schnoor AC, Gradert C, Schleupner M, Krahmer J, Tuczek F (2015) Z Anorg All Chem 641:83–90
49. Green LM, Meek DW (1990) Polyhedron 9:35–45
50. Dahlenburg L, Pietsch B (1986) Z Naturforsch B Anorg Chem Org Chem 41:70–75
51. Batke S, Kothe T, Haas M, Wadepohl H, Ballmann J (2016) Dalton Trans 45:3528–3540
52. Bujard M, Gouverneur V, Mioskowski C (1999) J Org Chem 64:2119–2123
53. Kostas ID (2001) J Organomet Chem 626:221–226
54. Stoffelbach F, Saurenz D, Poli R (2001) Eur J Inorg Chem:2699–2703
55. Owens BE, Poli R, Rheingold AL (1989) Inorg Chem 28:1456–1462
56. Poli R, Krueger ST, Mattamana SP, Dunbar KR, Hanhua Z (1998) Inorg Synth 32:198–203
57. Arduengo III AJ, Harlow RL, Kline M (1991) J Am Chem Soc 113:361–363

58. Enders D, Niemeier O, Henseler A (2007) Chem Rev 107:5606–5655
59. Scholl M, Trnka TM, Morgan JP, Grubbs RH (1999) Tetrahedron Lett 40:2247–2250
60. Herrmann WA, Köcher C (1997) Angew Chem 109:2256–2282; Angew Chem Int Ed (1997) 36:2162–2187
61. Fürstner A, Alcarazo M, Radkowski K, Lehmann CW (2008) Angew Chem 120:8426–8430; Angew Chem Int Ed (2008) 47:8302–8306
62. Dorta R, Stevens ED, Hoff CD, Nolan SP (2003) J Am Chem Soc 125:10490–10491
63. Hillier AC, Sommer WJ, Yong BS, Petersen JL, Cavallo L, Nolan SP (2003) Organometallics 22:4322–4326
64. Gradert C, Krahmer J, Sönnichsen FD, Näther C, Tuczek F (2013) Eur J Inorg Chem:3943–3955
65. Gradert C, Krahmer J, Sönnichsen FD, Näther C, Tuczek F (2014) J Organomet Chem 770:61–68
66. Gradert C, Stucke N, Krahmer J, Näther C, Tuczek F (2015) Chem A Eur J 21:1130–1137
67. Krahmer J, Broda H, Peters G, Näther C, Thimm W, Tuczek F (2011) Eur J Inorg Chem:4377–4386
68. Krahmer J, Peters G, Tuczek F (2014) Z Anorg Allg Chem 640:2834–2838
69. Söncksen L, Gradert C, Krahmer J, Näther C, Tuczek F (2013) Inorg Chem 52:6576–6589
70. Broda H, Hinrichsen S, Krahmer J, Näther C, Tuczek F (2014) Dalton Trans 43:2007–2012
71. Broda H, Krahmer J, Tuczek F (2014) Eur J Inorg Chem:3564–3571
72. Jacobsen H, Correa A, Costabile C, Cavallo L (2006) J Organomet Chem 691:4350–4358
73. Cotton FA, Kraihanzel CS (1962) J Am Chem Soc 84:4432–4438
74. Hahn FE, Jahnke MC, Pape T (2006) Organometallics 25:5927–5936
75. Lazarowych NJ, Morris RH, Ressner JM (1986) Inorg Chem 25:3926–3932
76. Yuki M, Miyake Y, Nishibayashi Y (2009) Organometallics 28:5821–5827
77. Yuki M, Midorikawa T, Miyake Y, Nishibayashi Y (2009) Organometallics 28:4741–4746
78. Schnöckel H, Schunck S (1987) Z Anorg Allg Chem 548:161–164
79. Brupbacher-Gatehouse B, Brupbacher T (1999) J Chem Phys 111:6300–6310
80. Niecke E, Engelmann M, Zorn H, Krebs B, Henkel G (1980) Angew Chem 92:738–739; Angew Chem Int Ed Engl (1980) 19:710–712
81. Niecke E, Zorn H, Krebs B, Henkel G (1980) Angew Chem 92:737–738; Angew Chem Int Ed Engl (1980) 19:709–710
82. Keck H, Kuchen W, Renneberg H, Terlouw JK, Visser HC (1991) Angew Chem 103:331–333; Angew Chem Int Ed (1991) 30:318–320
83. Klatt K, Stephan G, Peters G, Tuczek F (2008) Inorg Chem 47:6541–6550
84. Seitz T, Muth A, Huttner G (1994) Chem Ber 127:1837–1842
85. Fox MA, Campbell KA, Kyba EP (1981) Inorg Chem 20:4163–4165
86. Studt F, Tuczek F (2006) J Comput Chem 27:1278–1291
87. Muth A, Walter O, Huttner G, Asam A, Zsolnai L, Emmerich C (1994) J Organomet Chem 468:149–163
88. Janssen BC, Asam A, Huttner G, Sernau V, Zsolnai L (1994) Chem Ber 127:501–506
89. Poli R, Krueger ST, Mattamana SP, Dunbar KR, Hanhua Z (1998) Inorg Synth 32:198–203
90. Tolman CA (1977) Chem Rev 77:313–348
91. Brookhart M, Grant B, Volpe AF (1992) Organometallics 11:3920–3922
92. Hinrichsen S, Kindjajev A, Adomeit S, Krahmer J, Näther C, Tuczek F (2016) Inorg Chem 55:8712–8722
93. Card PJ, Hitz WD (1984) J Am Chem Soc 106:5348–5350
94. Walter O, Huttner G, Zsolnai L (1993) Z Naturforsch B Chem Sci 48:636–640
95. Hofacker P, Friebel C, Dehnicke K, Bäuml P, Hiller W, Strahle J (1989) Z Naturforsch B Chem Sci 44:1161–1166
96. Günther H (1972) Angew Chem 84:907–920; Angew Chem Int Ed Engl (1972) 11:861–874
97. Haymore BL, Hughes M, Mason J, Richards RL (1988) J Chem Soc Dalton Trans:2935–2940
98. Donovan-Mtsunzi S, Richards RL, Mason J (1984) J Chem Soc Dalton Trans:1329–1332